



# Recent Results of sub-PeV Gamma-Ray Observation with the Tibet AS $\gamma$ Experiment

Kazumasa KAWATA (ICRR, University of Tokyo)

For the Tibet AS $\gamma$  Collaboration





# Tibet AS $\gamma$ Collaboration



M. Amenomori<sup>1</sup>, S. Asano<sup>2</sup>, Y. W. Bao<sup>3</sup>, X. J. Bi<sup>4</sup>, D. Chen<sup>5</sup>, T. L. Chen<sup>6</sup>, W. Y. Chen<sup>4</sup>, Xu Chen<sup>4,5</sup>, Y. Chen<sup>3</sup>, Cirennima<sup>6</sup>, S. W. Cui<sup>7</sup>, Danzengluobu<sup>6</sup>, L. K. Ding<sup>4</sup>, J. H. Fang<sup>4,8</sup>, K. Fang<sup>4</sup>, C. F. Feng<sup>9</sup>, Zhaoyang Feng<sup>4</sup>, Z. Y. Feng<sup>10</sup>, Qi Gao<sup>6</sup>, A. Gomi<sup>11</sup>, Q. B. Gou<sup>4</sup>, Y. Q. Guo<sup>4</sup>, Y. Y. Guo<sup>4</sup>, Y. Hayashi<sup>12</sup>, H. H. He<sup>4</sup>, Z. T. He<sup>7</sup>, K. Hibino<sup>12</sup>, N. Hotta<sup>13</sup>, Haibing Hu<sup>6</sup>, H. B. Hu<sup>4</sup>, K. Y. Hu<sup>4,8</sup>, J. Huang<sup>4</sup>, H. Y. Jia<sup>10</sup>, L. Jiang<sup>4</sup>, P. Jiang<sup>5</sup>, H. B. Jin<sup>5</sup>, K. Kasahara<sup>14</sup>, Y. Katayose<sup>11</sup>, C. Kato<sup>2</sup>, S. Kato<sup>15</sup>, I. Kawahara<sup>11</sup>, T. Kawashima<sup>15</sup>, K. Kawata<sup>15</sup>, M. Kozai<sup>16</sup>, D. Kurashige<sup>11</sup>, Labaciren<sup>6</sup>, G. M. Le<sup>17</sup>, A. F. Li<sup>4,9,18</sup>, H. J. Li<sup>6</sup>, W. J. Li<sup>4,10</sup>, Y. Li<sup>5</sup>, Y. H. Lin<sup>4,8</sup>, B. Liu<sup>19</sup>, C. Liu<sup>4</sup>, J. S. Liu<sup>4</sup>, L. Y. Liu<sup>5</sup>, M. Y. Liu<sup>6</sup>, W. Liu<sup>4</sup>, X. L. Liu<sup>5</sup>, Y.-Q. Lou<sup>20,21,22</sup>, H. Lu<sup>4</sup>, X. R. Meng<sup>6</sup>, Y. Meng<sup>4,8</sup>, K. Munakata<sup>2</sup>, K. Nagaya<sup>11</sup>, Y. Nakamura<sup>15</sup>, Y. Nakazawa<sup>23</sup>, H. Nanjo<sup>1</sup>, C. C. Ning<sup>6</sup>, M. Nishizawa<sup>24</sup>, R. Noguchi<sup>11</sup>, M. Ohnishi<sup>15</sup>, S. Okukawa<sup>11</sup>, S. Ozawa<sup>25</sup>, L. Qian<sup>5</sup>, X. Qian<sup>5</sup>, X. L. Qian<sup>26</sup>, X. B. Qu<sup>27</sup>, T. Saito<sup>28</sup>, Y. Sakakibara<sup>11</sup>, M. Sakata<sup>29</sup>, T. Sako<sup>15</sup>, T. K. Sako<sup>15</sup>, T. Sasaki<sup>12</sup>, J. Shao<sup>4,9</sup>, M. Shibata<sup>11</sup>, A. Shiomi<sup>23</sup>, H. Sugimoto<sup>30</sup>, W. Takano<sup>12</sup>, M. Takita<sup>15</sup>, Y. H. Tan<sup>4</sup>, N. Tateyama<sup>12</sup>, S. Torii<sup>31</sup>, H. Tsuchiya<sup>32</sup>, S. Udo<sup>12</sup>, H. Wang<sup>4</sup>, Y. P. Wang<sup>6</sup>, Wangdui<sup>6</sup>, H. R. Wu<sup>4</sup>, Q. Wu<sup>6</sup>, J. L. Xu<sup>5</sup>, L. Xue<sup>9</sup>, Z. Yang<sup>4</sup>, Y. Q. Yao<sup>5</sup>, J. Yin<sup>5</sup>, Y. Yokoe<sup>15</sup>, N. P. Yu<sup>5</sup>, A. F. Yuan<sup>6</sup>, L. M. Zhai<sup>5</sup>, C. P. Zhang<sup>5</sup>, H. M. Zhang<sup>4</sup>, J. L. Zhang<sup>4</sup>, X. Zhang<sup>3</sup>, X. Y. Zhang<sup>9</sup>, Y. Zhang<sup>4</sup>, Yi Zhang<sup>33</sup>, Ying Zhang<sup>4</sup>, S. P. Zhao<sup>4</sup>, Zhaxisangzhu<sup>6</sup>, X. X. Zhou<sup>10</sup> and Y. H. Zou<sup>4,8</sup>

1 Department of Physics, Hiroshima Univ., Japan.

2 Department of Physics, Shinshu Univ., Japan.

3 School of Astronomy and Space Science, Nanjing Univ., China.

4 Key Laboratory of Particle Astrophysics, Institute of High Energy Physics, CAS, China.

5 National Astronomical Observatories, CAS, China.

6 Department of Mathematics and Physics, Tibet Univ., China.

7 Department of Physics, Hebei Normal Univ., China.

8 Univ. of Chinese Academy of Sciences, China.

9 Institute of Frontier and Interdisciplinary Science and Key Laboratory of Particle Physics and Particle Irradiation (MOE), Shandong Univ., China.

10 Institute of Modern Physics, SouthWest Jiaotong Univ., China.

11 Faculty of Engineering, Yokohama National Univ., Japan.

12 Faculty of Engineering, Kanagawa Univ., Japan.

13 Faculty of Education, Utsunomiya Univ., Japan.

14 Faculty of Systems Engineering, Shibaura Institute of Technology, Japan.

15 Institute for Cosmic Ray Research, Univ. of Tokyo, Japan.

16 Polar Environment Data Science Center, Joint Support-Center for Data Science Research, Research Organization of Information and Systems, Japan.

17 National Center for Space Weather, China Meteorological Administration, China.

18 School of Information Science and Engineering, Shandong Agriculture Univ., China.

19 Department of Astronomy, School of Physical Sciences, Univ. of Science and Technology of China, China.

20 Department of Physics and Tsinghua Centre for Astrophysics (THCA), Tsinghua Univ., China.

21 Tsinghua Univ.-National Astronomical Observatories of China (NAOC) Joint Research Center for Astrophysics, Tsinghua Univ., China.

22 Department of Astronomy, Tsinghua Univ., China.

23 College of Industrial Technology, Nihon Univ., Japan.

24 National Institute of Informatics, Japan.

25 National Institute of Information and Communications Technology, Japan.

26 Department of Mechanical and Electrical Engineering, Shangdong Management Univ., China.

27 College of Science, China Univ. of Petroleum, China.

28 Tokyo Metropolitan College of Industrial Technology, Japan.

29 Department of Physics, Konan Univ., Japan.

30 Shonan Institute of Technology, Japan.

31 Research Institute for Science and Engineering, Waseda Univ., Japan.

32 Japan Atomic Energy Agency, TJapan.

33 Key Laboratory of Dark Matter and Space Astronomy, Purple Mountain Observatory, CAS, China.

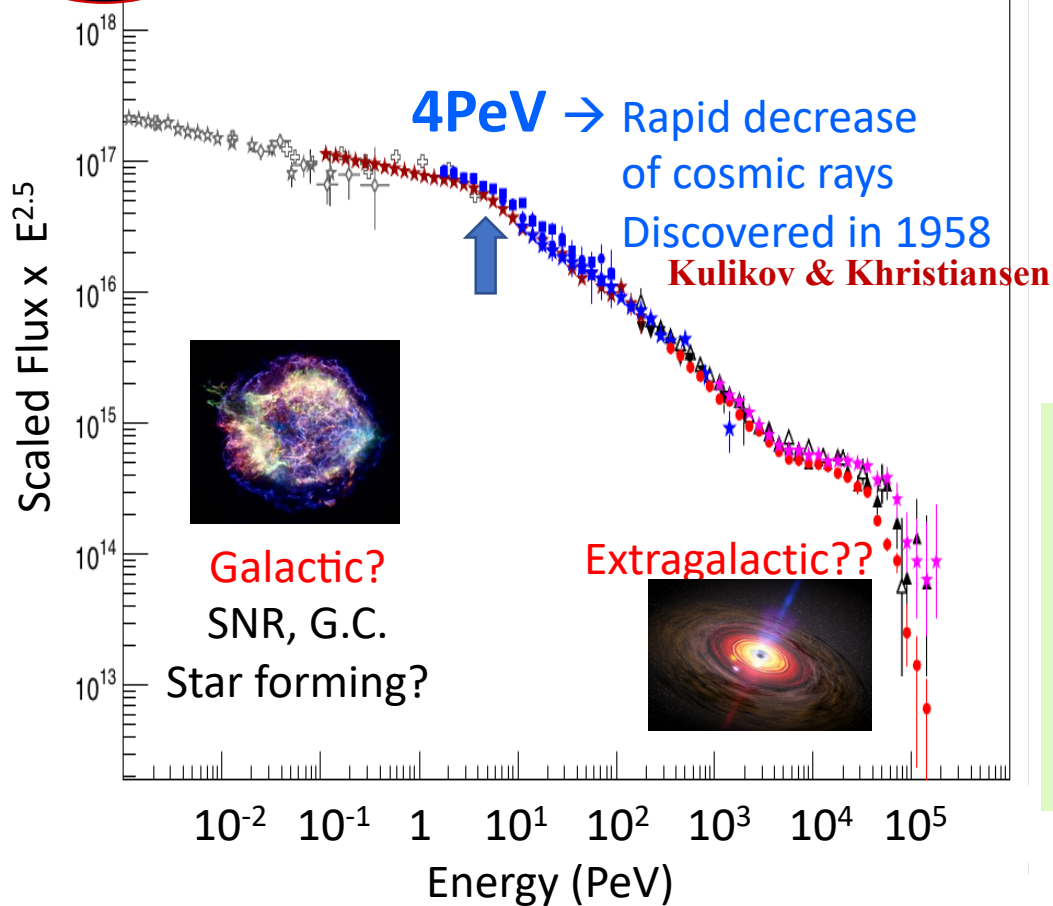


# Outline

1. Introduction
2. Tibet AS $\gamma$  Experiment
3. Galactic Diffuse Gamma Rays
4. PeVatron Candidates
5. Summary



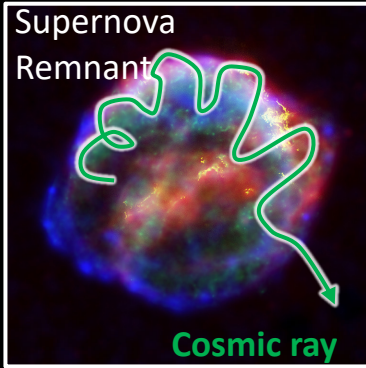
# Introduction



- ❖ Wide energy range
- ❖ Main component is proton
- ❖ Rate decreases to 1/100 when energy is 10 times higher

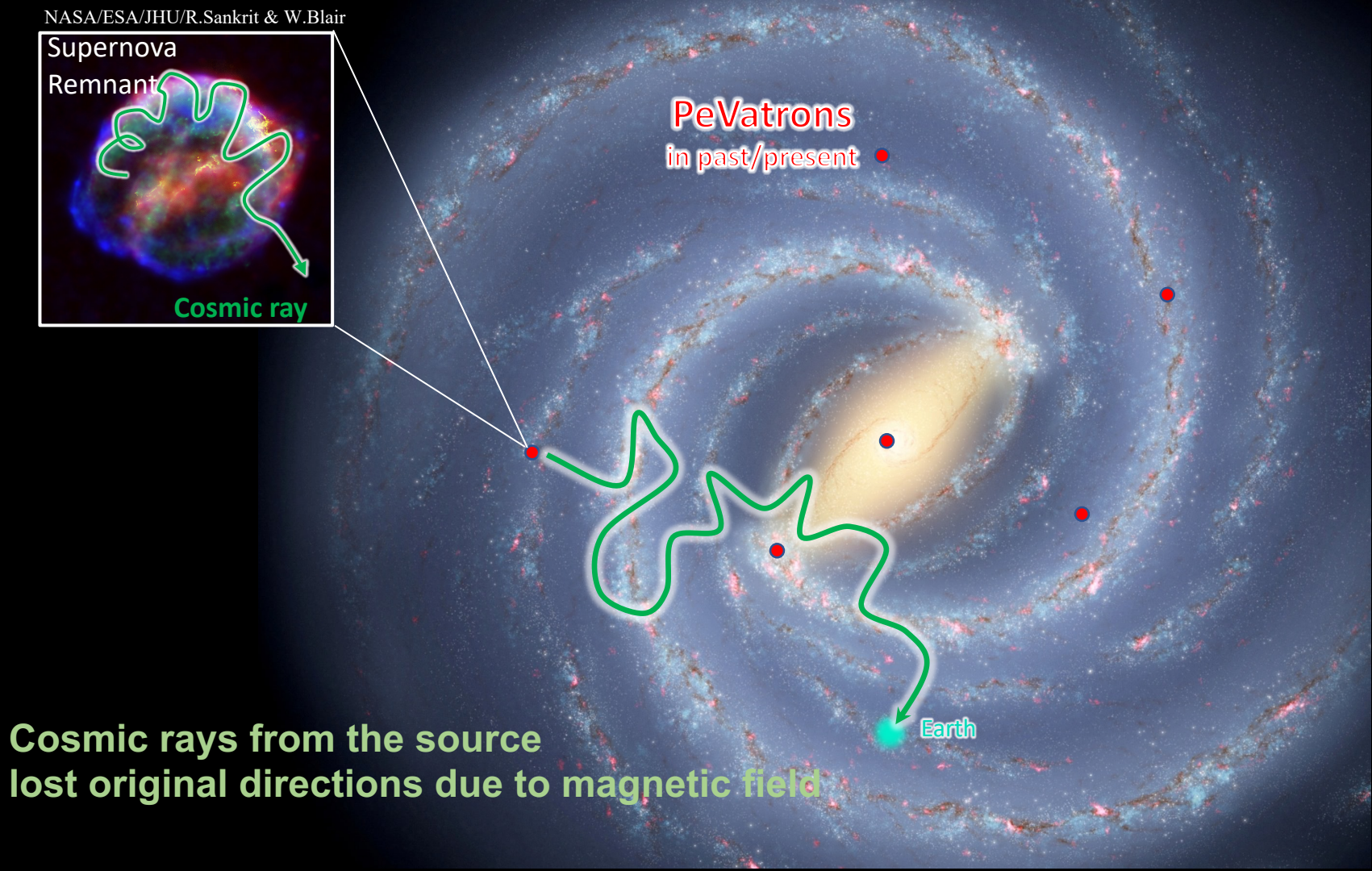
As an open question,  
Did/Do “PeVatrons” really exist in  
our Galaxy?

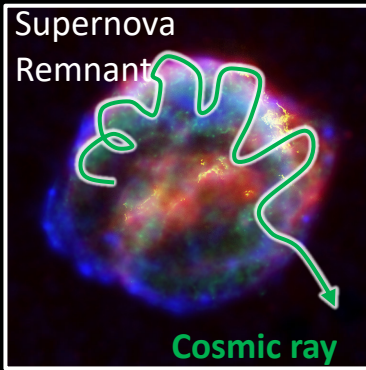
PeVatron: Cosmic super-accelerators  
can accelerate to Peta electron volt



PeVatrons  
in past/present

Cosmic rays from the source  
lost original directions due to magnetic field





PeVatrons

in past/present



Sub-PeV gamma ray

Earth

Cosmic rays interact with  
interstellar gas, and produce  $\gamma$  rays



( $\gamma$ -ray energy is  $\sim 10\%$  of cosmic ray's)  $\rightarrow$  sub-PeV gamma rays

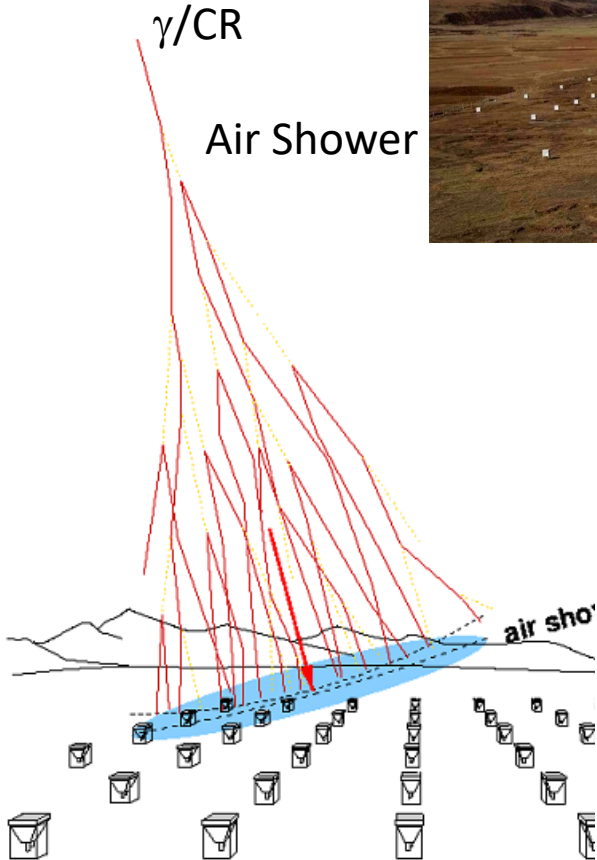


# Tibet Air Shower Array



$\gamma$ /CR

Air Shower



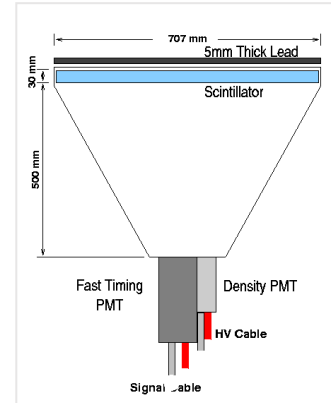
Air Shower Array

□ Site: Tibet ( $90.522^{\circ}\text{E}$ ,  $30.102^{\circ}\text{N}$ ) 4,300 m a.s.l.

## Present Performance

- ✓ # of detectors  $0.5 \text{ m}^2 \times 597$
- ✓ Covering area  $\sim 65,700 \text{ m}^2$
- ✓ Angular resolution  $\sim 0.5^{\circ}$  @  $10 \text{ TeV } \gamma$   
 $\sim 0.2^{\circ}$  @  $100 \text{ TeV } \gamma$
- ✓ Energy resolution  $\sim 40\%$  @  $10 \text{ TeV } \gamma$   
 $\sim 20\%$  @  $100 \text{ TeV } \gamma$

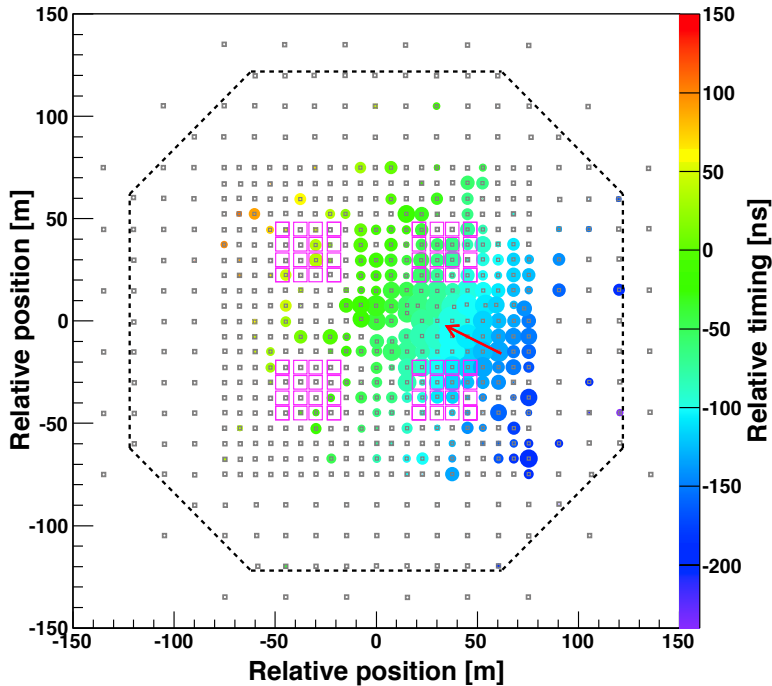
→ Observation of secondary (mainly  $e^{\pm}, \gamma$ ) in AS  
 Primary energy : 2<sup>nd</sup> particle densities  
 Primary direction : 2<sup>nd</sup> relative timings





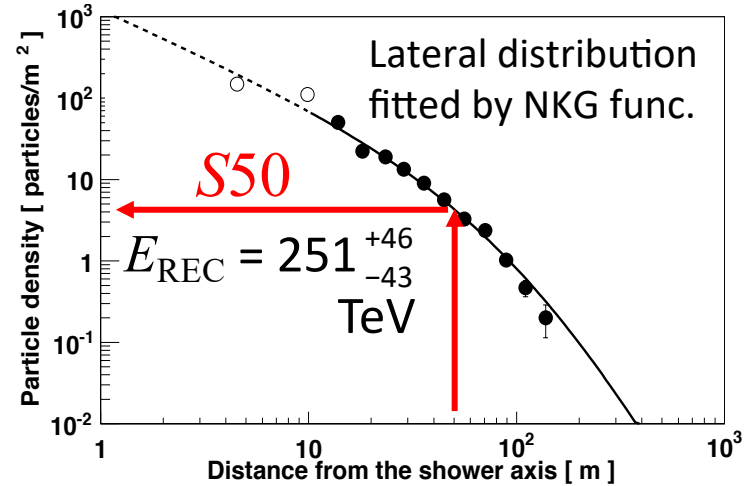
# Air Shower Reconstruction

Gamma-ray candidate event



circle size  $\propto \log(\# \text{ of detected particles})$   
 circle color  $\propto$  relative timing [ns]

*Amenomori +, PRL 123, 051101 (2019)*



*S50 improves  $E$  resolutions (10 - 1000 TeV)*  
 $\rightarrow \sim 40\% @ 10 \text{ TeV} , \sim 20\% @ 100 \text{ TeV}$

*Kawata+, Experimental Astronomy 44, 1 (2017)*

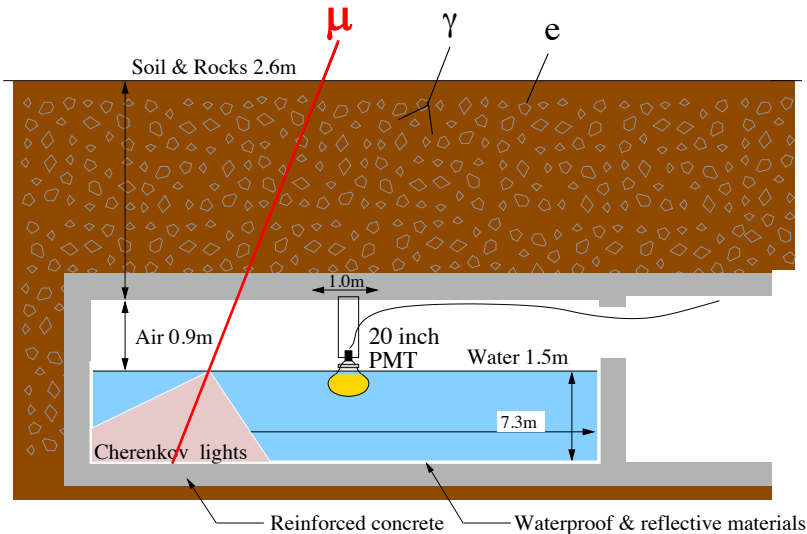
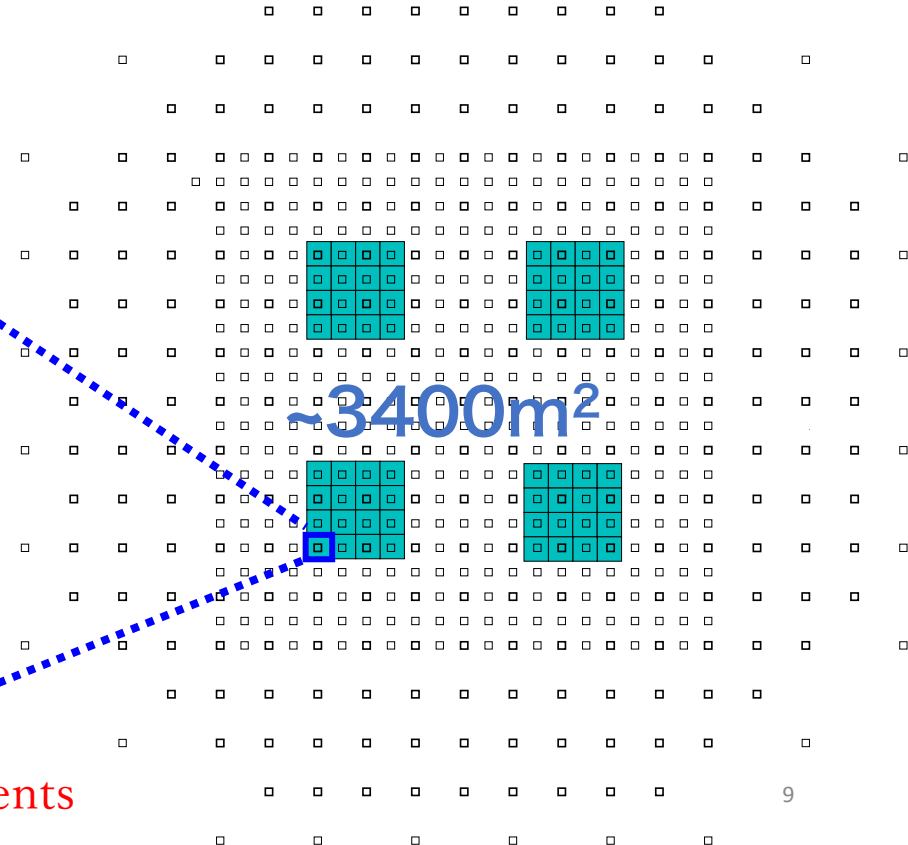




# Underground WC Muon Detectors

- ✓ 4 pools, 16 units / pool
- ✓ 54 m<sup>2</sup> in area × 1.5m in depth / unit
- ✓ 20"ΦPMT (HAMAMATSU R3600)
- ✓ Concrete pools + white Tyvek sheets
- ✓ 2.4m soil overburden ( $\sim 515\text{g/cm}^2 \sim 9X_0$ )

Measurement of # of  $\mu$  in AS  $\rightarrow \gamma$  / CR discrimination  
DATA: February 2014 - May 2017 **Live time: 719 days**

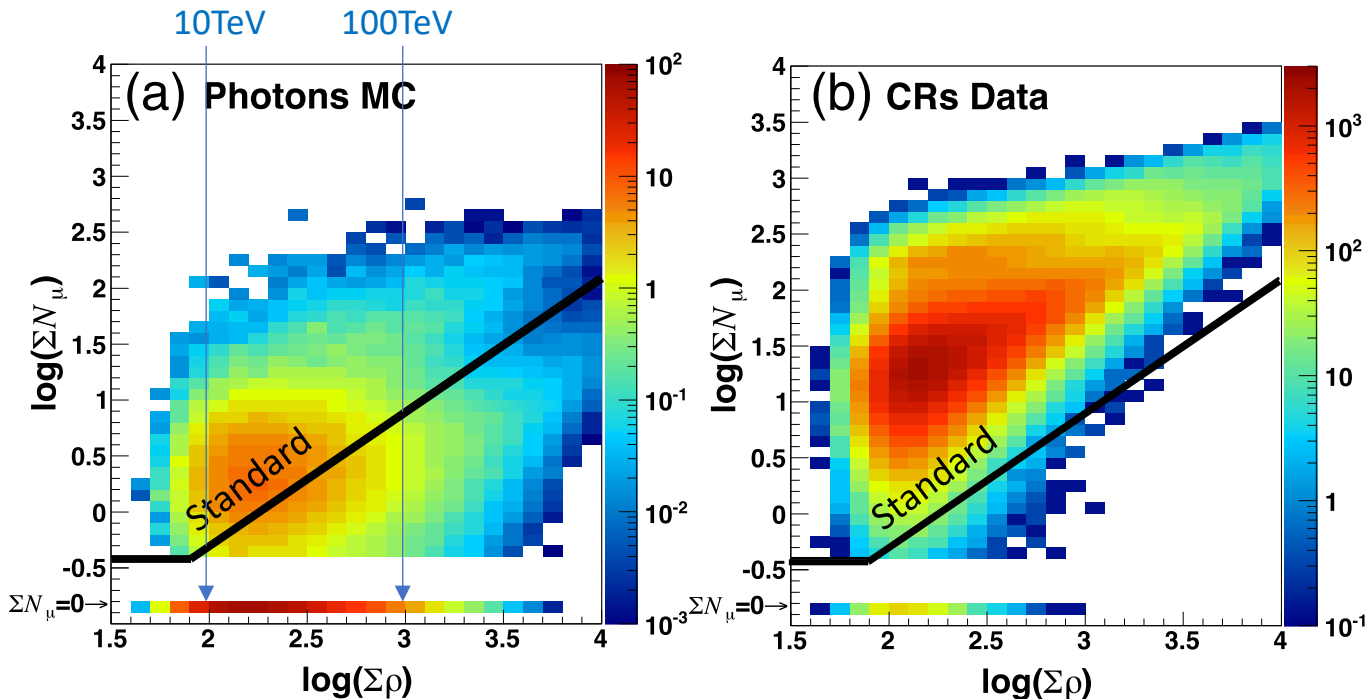


→ Succeeded in rejecting by  $>99.9\%$  CR events



# Muon Cut Condition (Standard)

Standard muon cut :  $\Sigma N_{\mu} < 2.1 \times 10^{-3} \Sigma \rho^{1.2}$  → Optimized for the gamma-ray point-like source

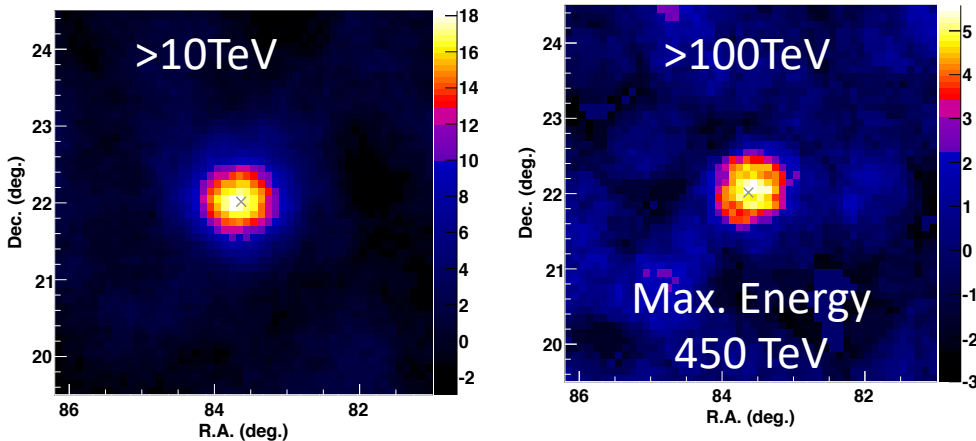


Gamma Survival ratio : ~90% by MC sim (>100TeV) CR Survival ratio :  $\sim 10^{-3}$  (>100TeV)



# UHE $\gamma$ -rays from the Crab Nebula (2019)

*Amenomori et al., PRL 123, 051101 (2019)*

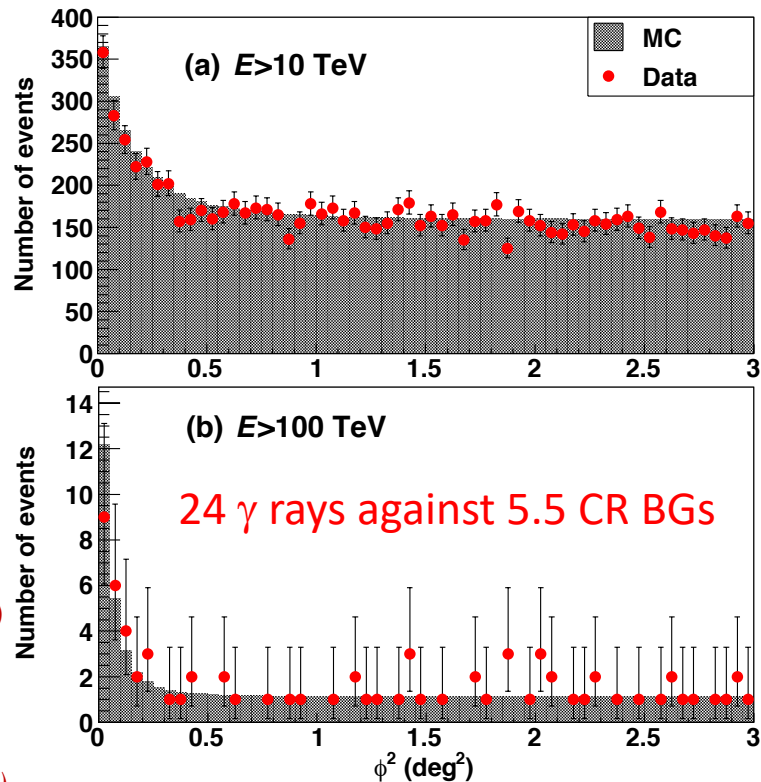


**First Detection of Sub-PeV  $\gamma$  ( $5.6\sigma$ )**

Other detected sources in 100 TeV region

- ✓ G106.3+2.7 *Amenomori et al., Nat. Astron, 5, 460 (2021)*
- ✓ Cygnus OB1 *Amenomori et al., PRL, 127, 031102 (2021)*
- ✓ Cygnus OB2
- ✓ HESS J1843-033 *Amenomori et al., ApJ, 932, 120 (2022)*
- ✓ HESS J1849-000 *Accepted (2023)*

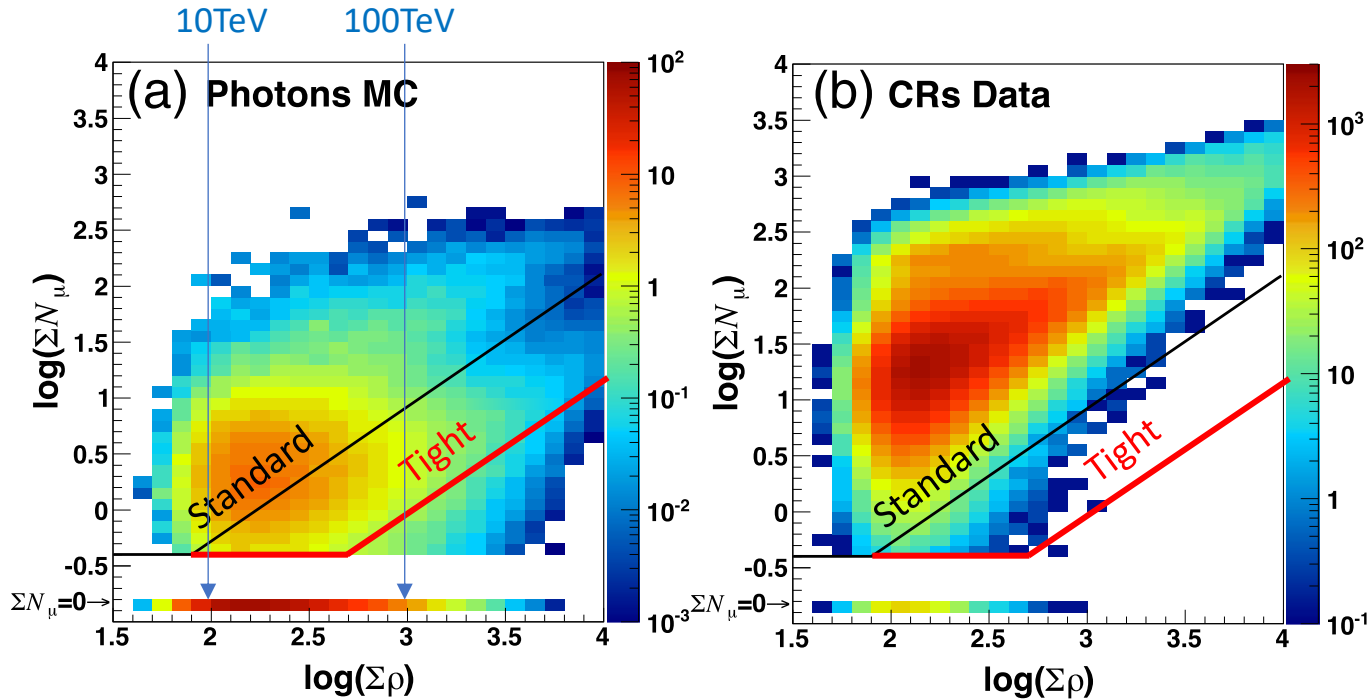
## Data vs MC





# Muon Cut Condition (Tight) for Diffuse $\gamma$

Tight muon cut :  $\Sigma N_{\mu} < 2.1 \times 10^{-4} \Sigma \rho^{1.2}$  → One order magnitude tighter than the Crab analysis



Gamma Survival ratio :  $\sim 30\%$  by MC sim ( $>398\text{TeV}$ ) CR Survival ratio :  $\sim 10^{-6}$  ( $>398\text{TeV} = 10^{2.6}\text{TeV}$ )



# $\gamma$ -ray-like event Distribution

Gamma-ray-like events  
after the tight muon cut  
in the equatorial coordinates

Blue points:

Experimental data

Red plus marks:

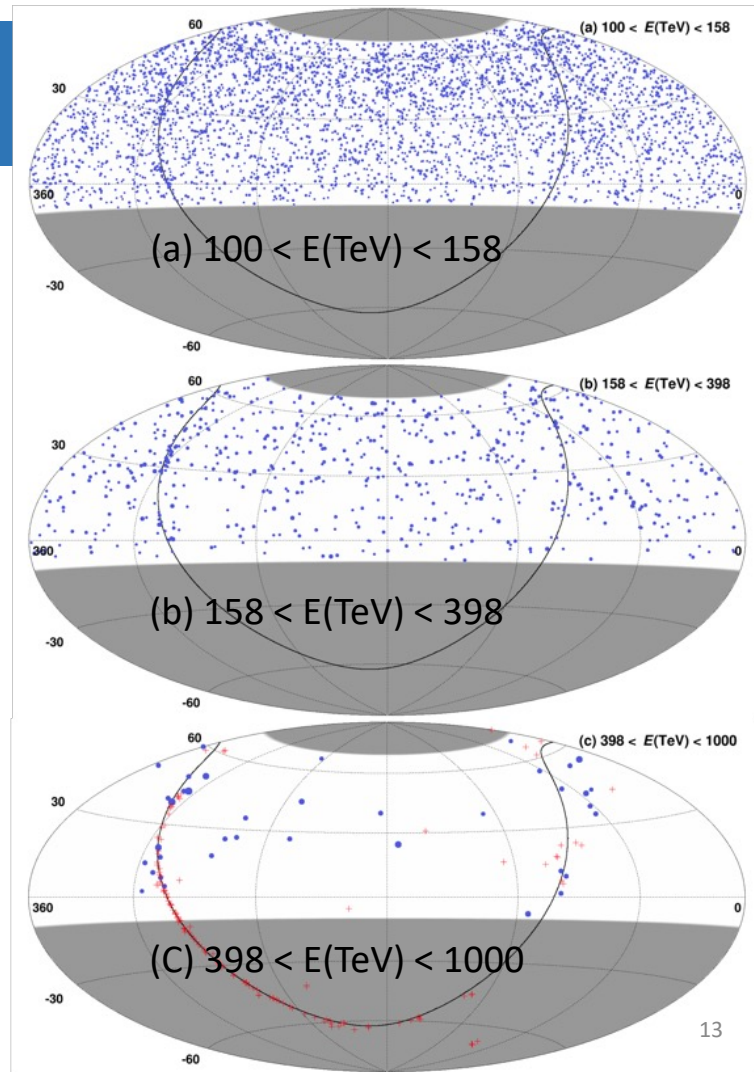
known Galactic TeV sources

$>398$  TeV ( $10^{2.6}$  TeV)

38 events in our FoV

23 events in  $|b| < 10^\circ$

16 events in  $|b| < 5^\circ$





# Latitude Profile

6.6 $\sigma$

*Amenomori et al., PRL 126, 141101 (2021)*

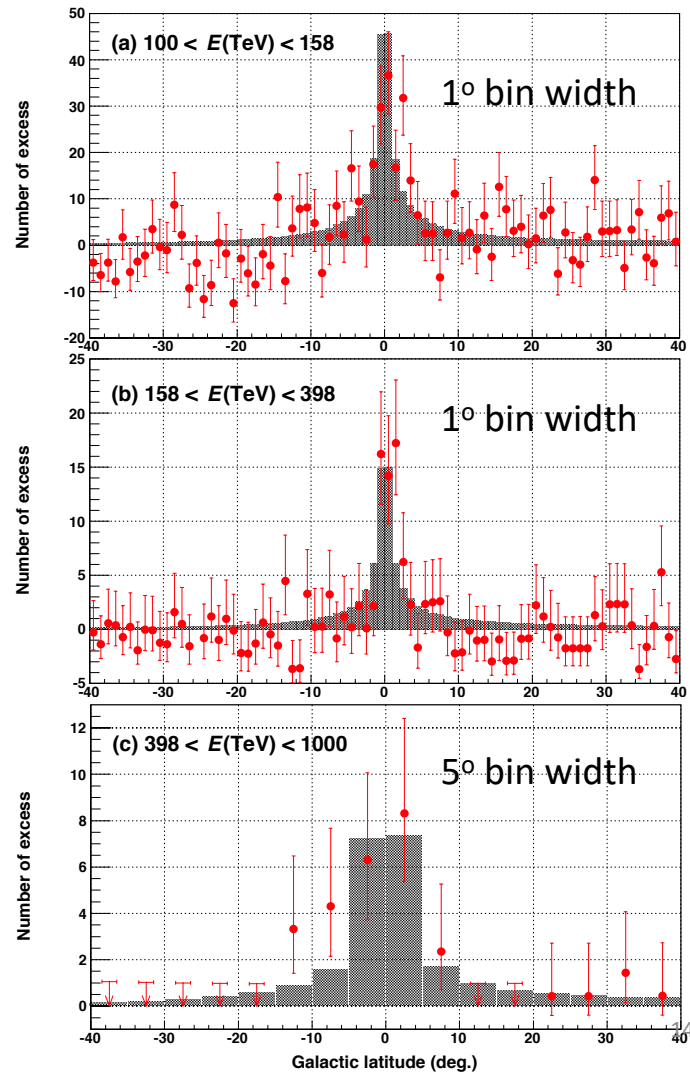
Red points:  
experimental data across  
our FoV ( $22^\circ < l < 225^\circ$ )  
including source contribution

5.1 $\sigma$

Gray shade histogram:  
Model by Lipari and Vernetto

*Lipari & Vernetto, PRD 98, 043003 (2018)*

5.9 $\sigma$





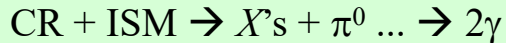
# Energy Spectrum of UHE Diffuse $\gamma$ Rays

*Amenomori et al., PRL 126, 141101 (2021)*

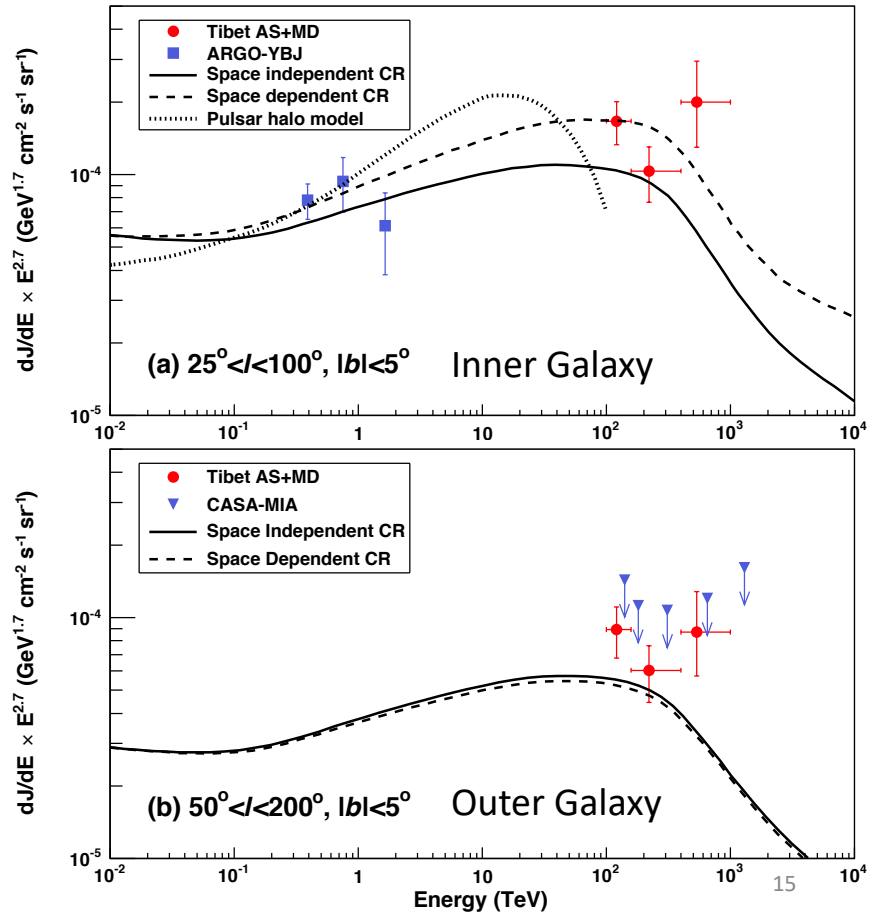
After excluding the contribution from the known TeV sources (within 0.5 degrees) listed in the TeV source catalog



The measured fluxes are overall consistent with Lipari's diffuse gamma model assuming the hadronic cosmic ray origin.



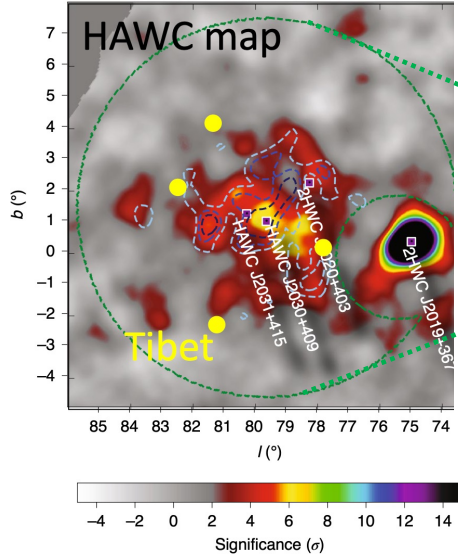
*Lipari & Vernetto, PRD 98, 043003 (2018)*



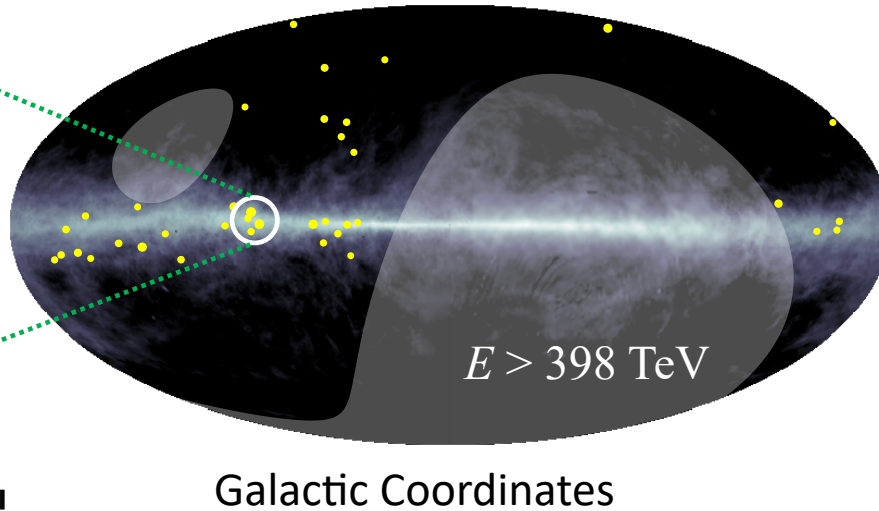


# PeVatron Candidate: Cygnus Cocoon

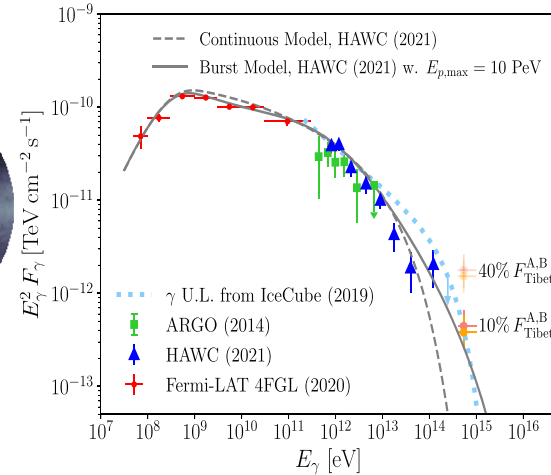
*Abeysekara et al.,  
Nature Astronomy (2021)*



*Amenomori et al., PRL 126, 141101 (2021)*



*Fang & Murase,  
ApJ, 919, 93 (2021)*



4 events above 398 TeV detected within 4°-radius-circle from the **Cygnus cocoon** which is claimed as an extended source by the ARGO-YBJ/HAWC/LHAASO and also proposed as a candidate of the PeVatrons.





# LHAASO Diffuse Gamma Rays

*Z. Cao et al. (LHAASO Collob.) PRL, 131, 151001 (2023)*

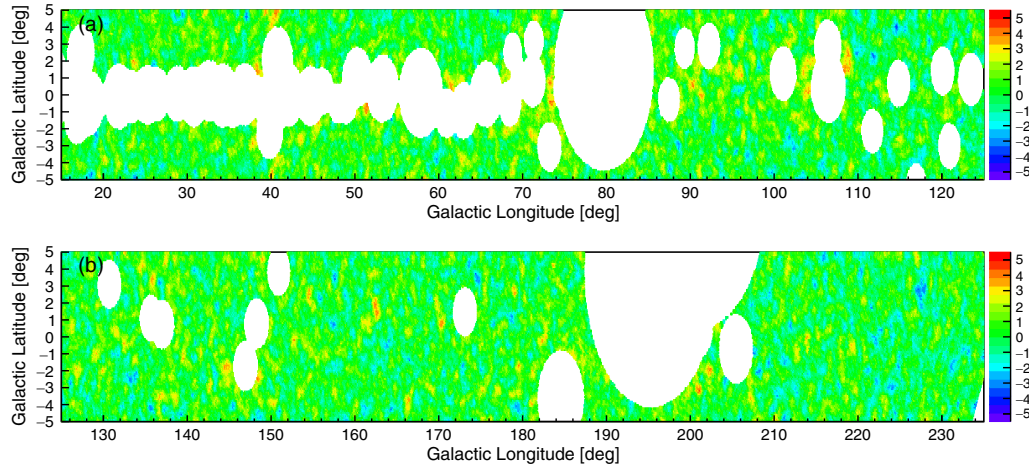
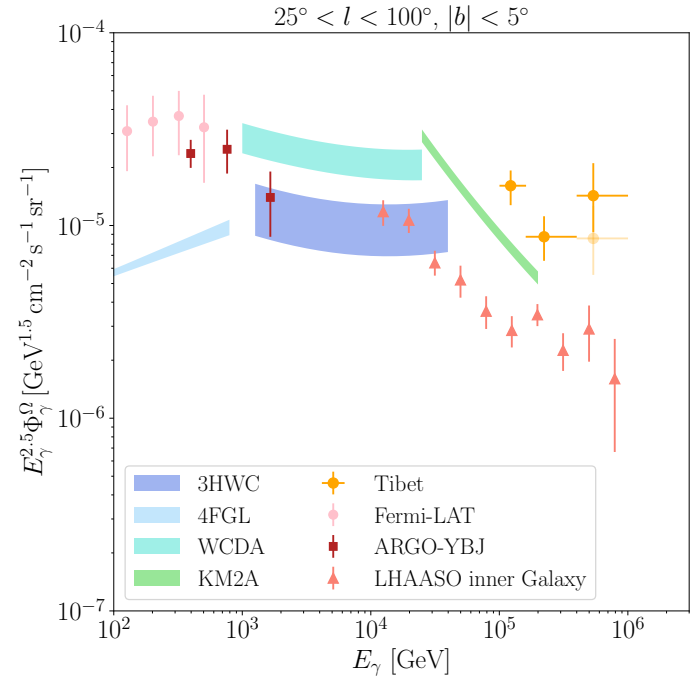


FIG. 1. The significance maps in Galactic coordinate of the inner Galaxy region [panel (a)] and outer Galaxy region [panel (b)] above 25 TeV after masking the resolved KM2A and TeVCat sources.

LHAASO flux: a few times lower than Tibet flux,  
but not directly compared, due to the large  
masked regions by LHAASO.

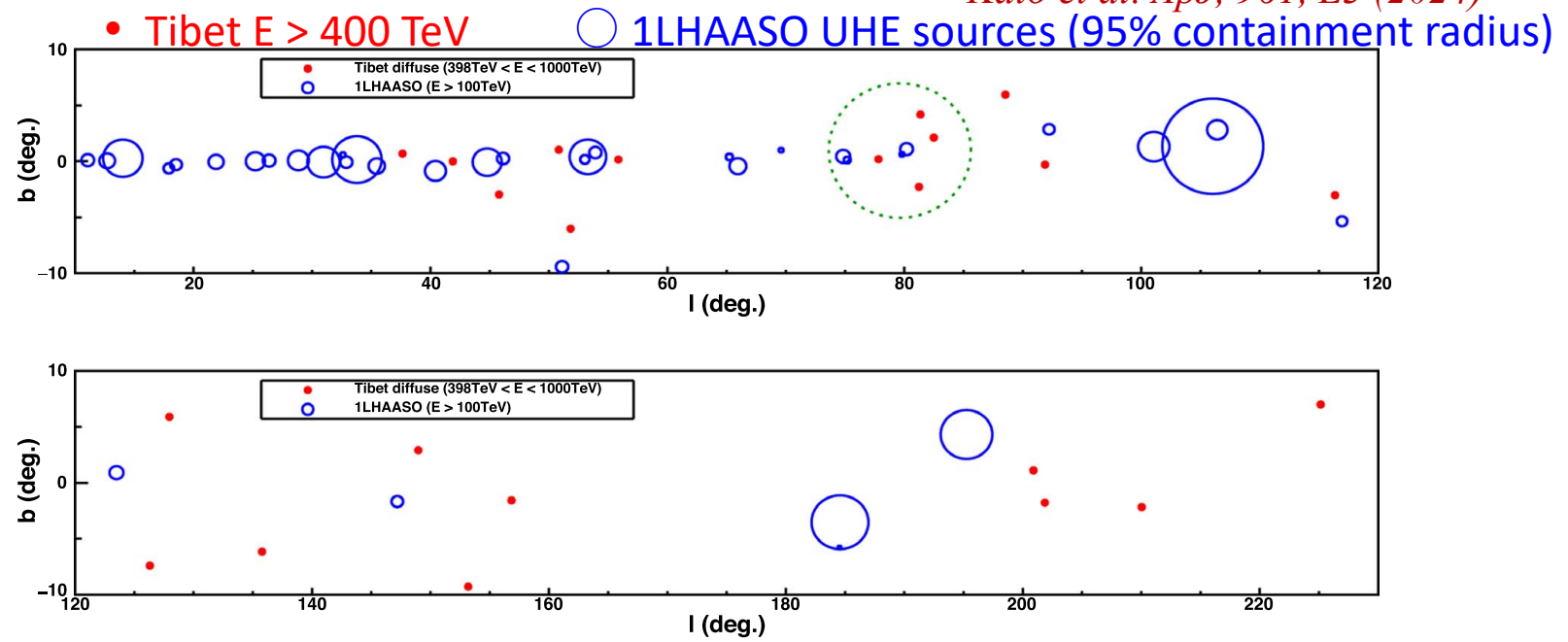
*K. Fang & K. Murase, ApJ, 957, L6 (2023)*





# 1LHAASO Catalog and Tibet UHE Diffuse Events

*Kato et al. ApJ, 961, L3 (2024)*



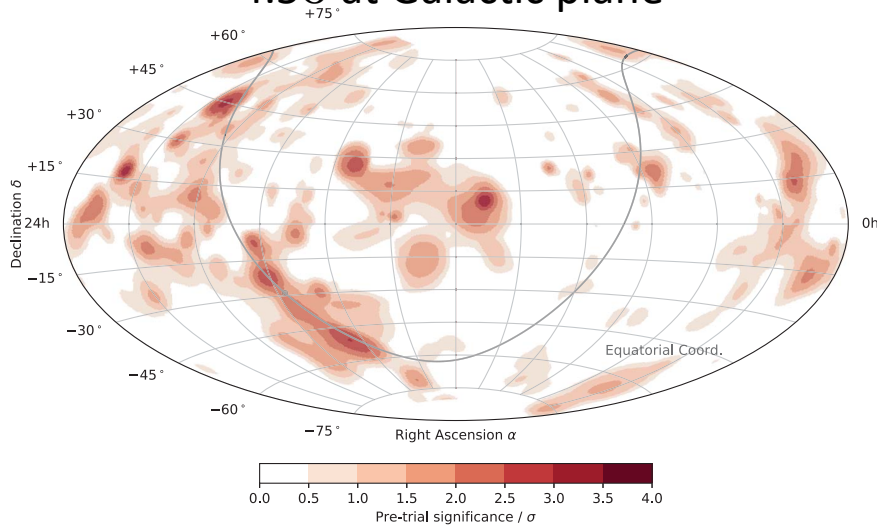
Tibet Galactic diffuse gamma rays above 400 TeV:  
do NOT originate from 1LHAASO UHE (>100 TeV) sources.



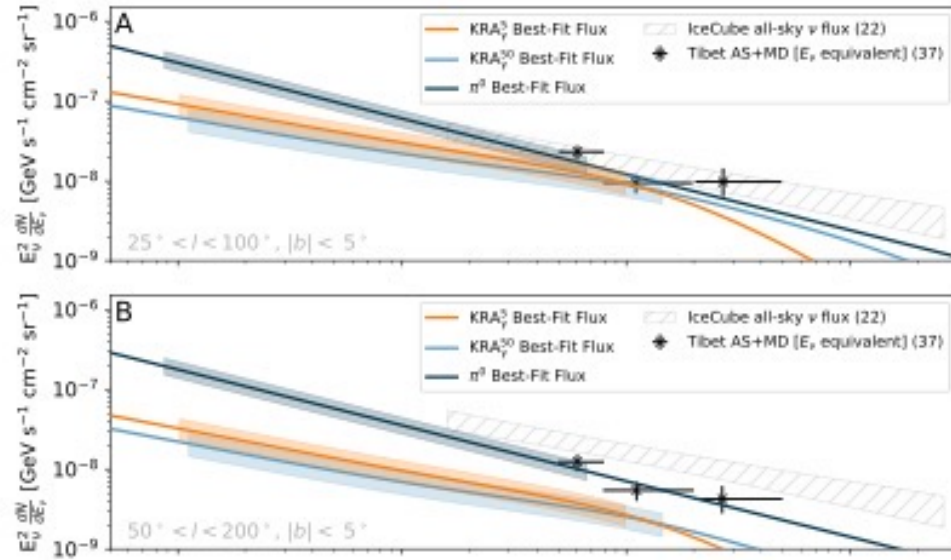
# IceCube Diffuse Neutrinos

*IceCube Collaboration: Science, 380, 1338 (2023)*

4.5 $\sigma$  at Galactic plane



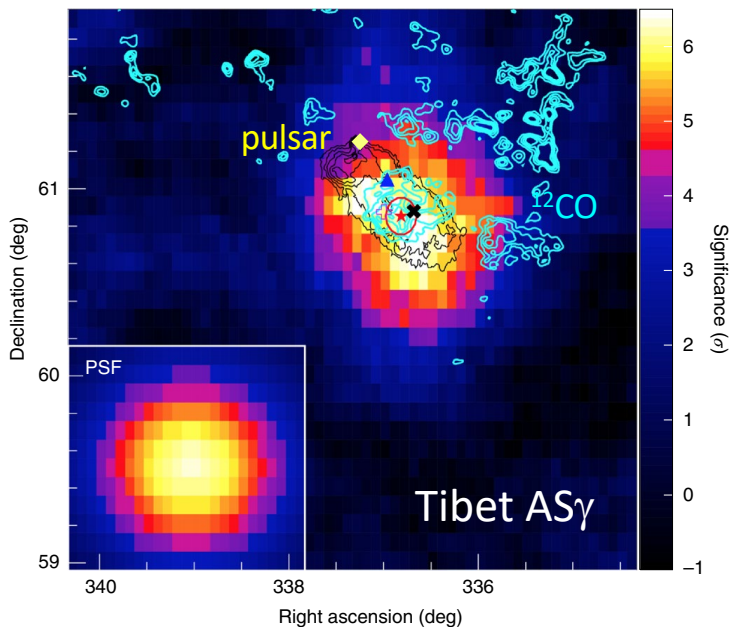
Comparison with Tibet diffuse  $\gamma$ -rays



IceCube  $\nu$  flux smoothly connects to the  $\nu$  flux estimated from the Tibet sub-PeV  $\gamma$ -ray flux, assuming  $\pi^0$ -model best-fit flux supporting cosmic-ray origin of Tibet sub-PeV galactic diffuse  $\gamma$  rays.

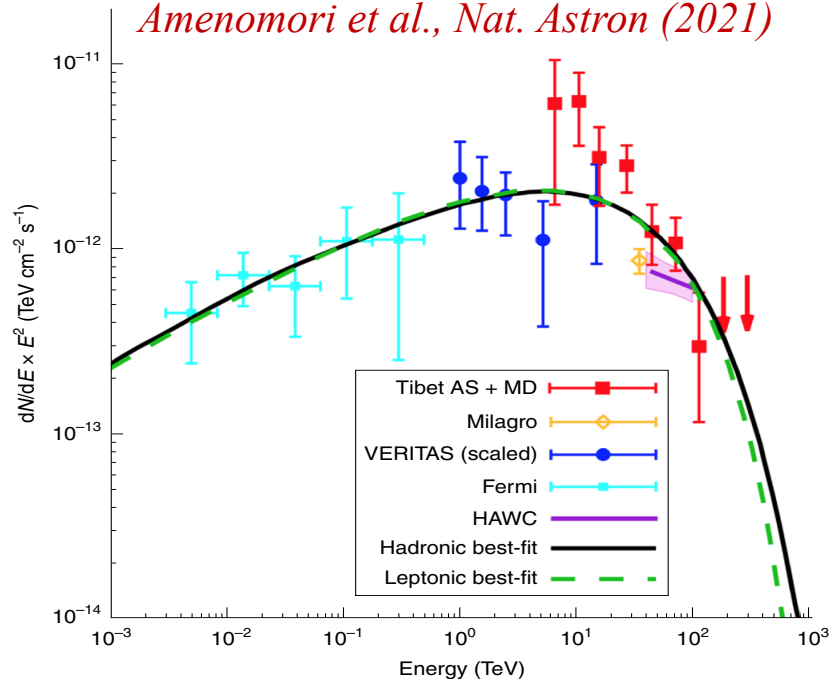


# PeVatron Candidate: SNR G106.3+2.7



Detected by  
VERITAS,  
HAWC,  
Tibet AS $\gamma$ ,  
MAGIC,  
LHAASO

*Amenomori et al., Nat. Astron (2021)*



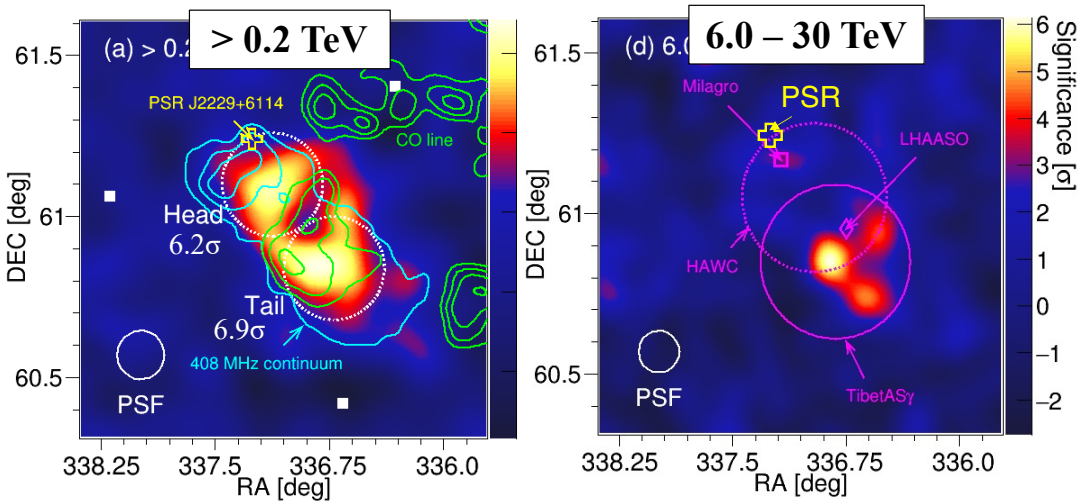
- ✓ Spectrum extends beyond 100 TeV (HAWC, Tibet AS $\gamma$ , LHAASO)
- ✓ Shell-type SNR near the pulsar ( $t_{\text{age}} \sim 10 \text{ kyr?}$ ,  $d = 800 \text{ pc?}$ )
- ✓ Extended  $\gamma$ -ray excess ( $\sigma_{\text{EXT}} = 0.24^\circ \pm 0.10^\circ$ )
- ✓  $\gamma$ -ray excess is coincident with the molecular clouds (MCs) and SNR, not pulsar

$$E_{p,\text{cut}} = \sim 500 \text{ TeV}$$

$$W_p = \sim 5 \times 10^{47} \text{ erg} \quad (>1 \text{ GeV})$$

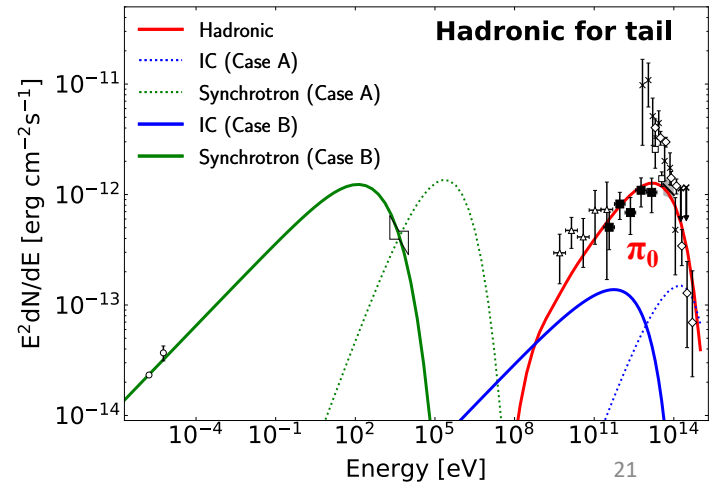
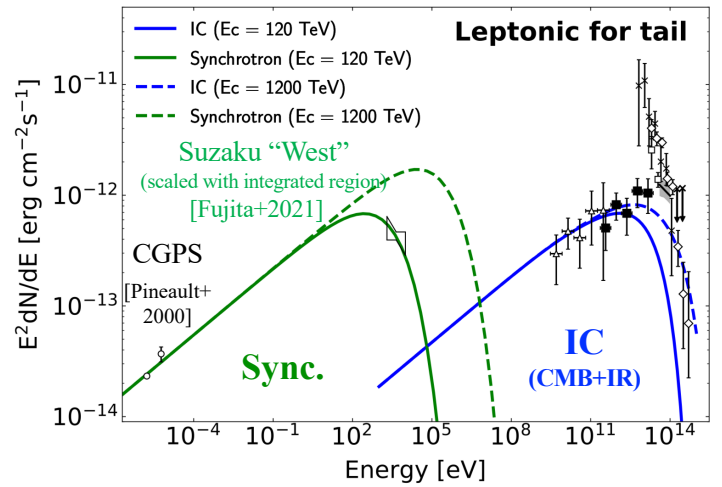


# MAGIC: SNR G106.3+2.7



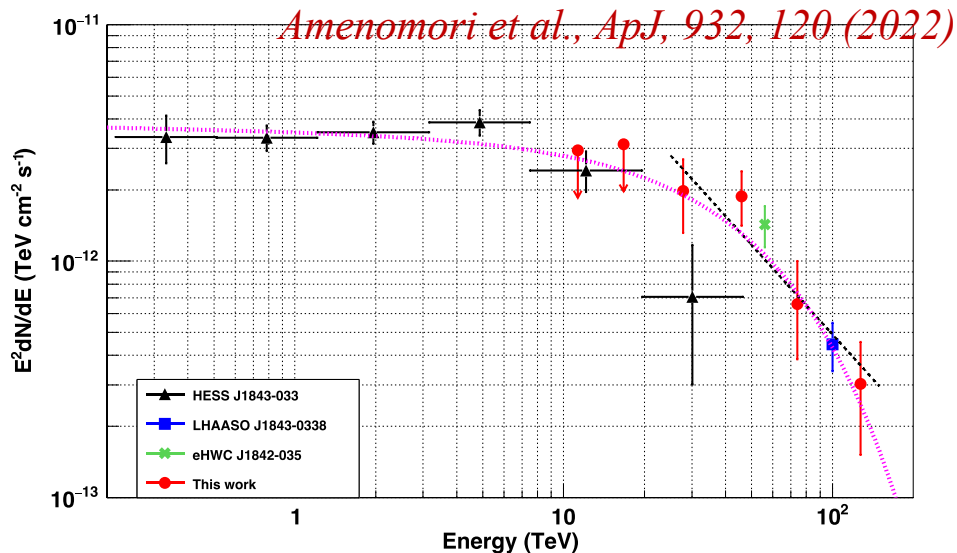
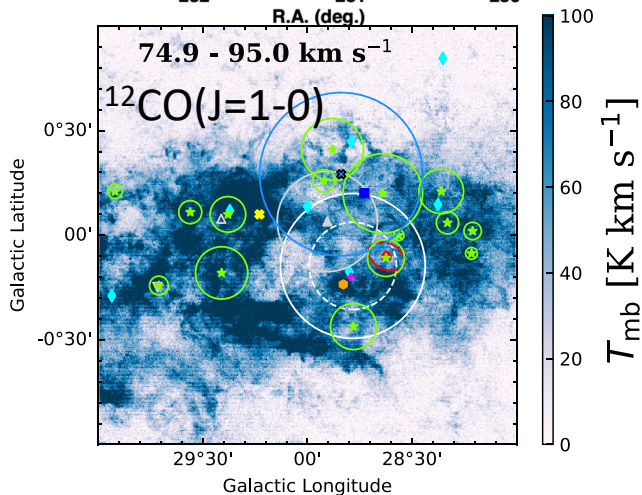
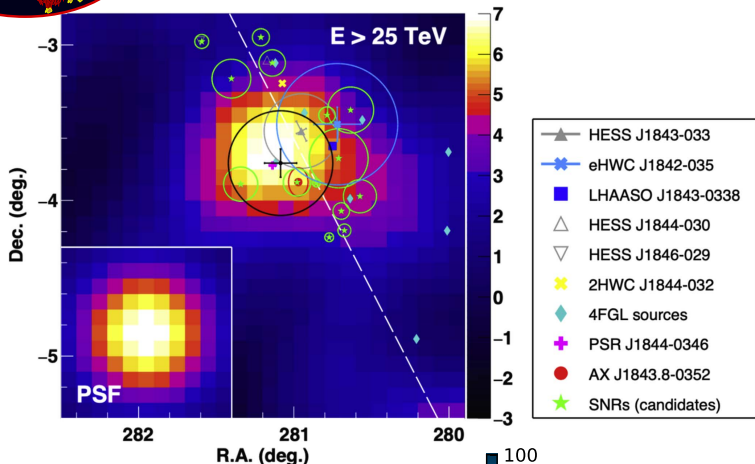
- ✓ HE emissions are consistent with Tibet ASy
- ✓ SED for tail region favors hadronic model

*Abe et al. (MAGIC Collab.), A&A, 671, 12 (2023)*  
*Oka et al. (MAGIC Collab.), CTA workshop*





# PeVatron Candidate: HESS J1843-033



Candidate sources ( $T_{\text{age}}=2.7\text{kyr?}$ ,  $d=9.6\text{kpc}$ )

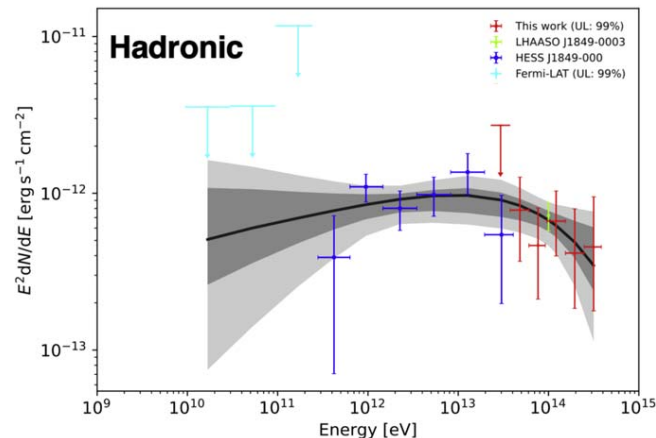
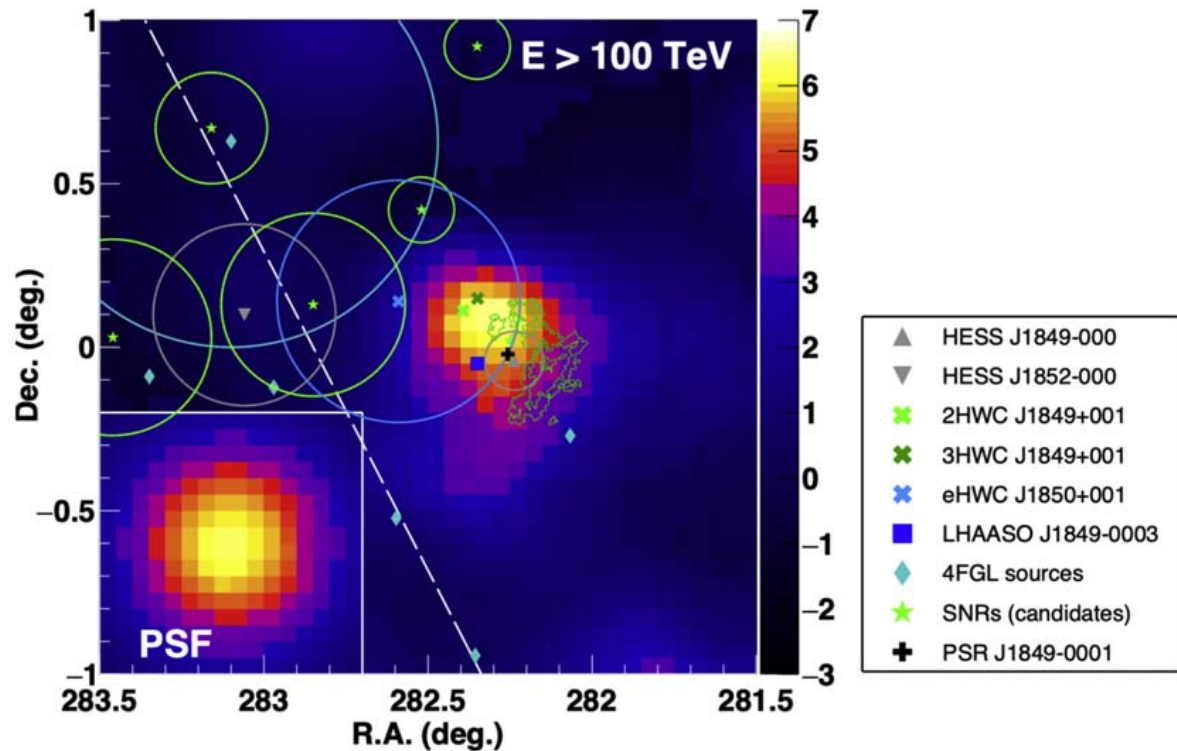
- ✓ Shell-type SNR G28.6+0.1? or PSR J1844-00346?
  - ✓ Extended  $\gamma$ -ray excess ( $\sigma_{\text{EXT}}=0.34^\circ \pm 0.12^\circ$ )
  - ✓  $\gamma$ -ray excess is coincident with the MCs
  - ✓ Proton cutoff:  $\sim 500 \text{ TeV}$  assuming the Hadronic model
- $W_p = \sim 6 \times 10^{49} \text{ erg } (>1\text{TeV})$



# PeVatron Candidate: HESS J1849-000

*Amenomori et al., ApJ, 954, 200 (2023)*

- ✓ A middle-aged PWN ( $T_{\text{age}}=42.9\text{kyr}$ ,  $d=7\text{kpc}$ )
- ✓  $\gamma$ -ray excess is coincident with the MCs

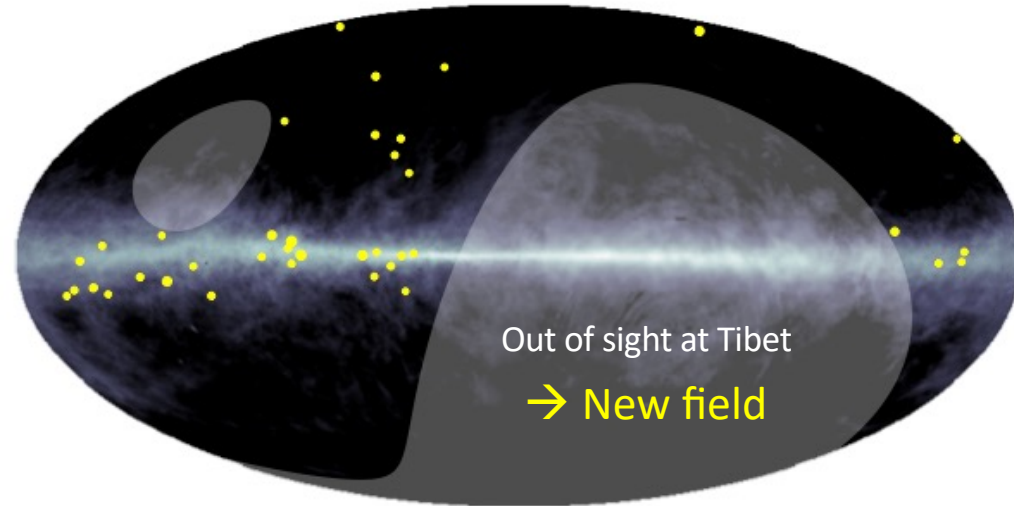


- ✓ Proton cutoff  $\sim 5$  PeV  
assuming the Hadronic model  
 $W_p = \sim 1.1 \times 10^{49}$  erg ( $>1\text{TeV}$ )
- ✓ Spectrum can be also modeled  
with the Leptonic scenario (IC)

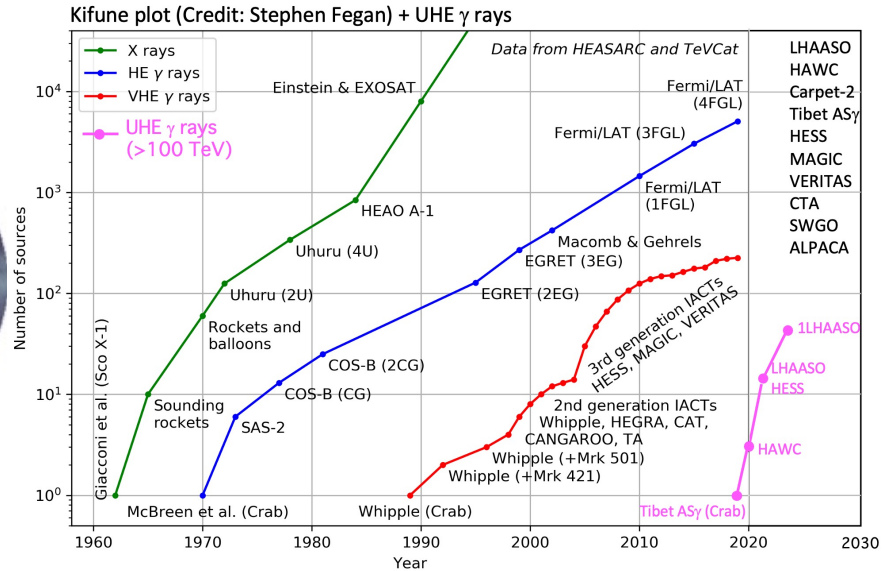


# Projects in the Southern Hemisphere

UHE diffuse gamma rays



>40 UHE sources



Draw the "Kifune" plot - the integral number of high energy sources detected as a function of year - in the style of a plot developed by Tadashi Kifune (for example <http://adsabs.harvard.edu/abs/1996NCimC..19..953K>). The data for the number of X-ray and HE (GeV) gamma-ray sources come from a page on HEASARC maintained by Stephen A. Drake (retrieved 2017-09-28) : [https://heasarc.gsfc.nasa.gov/docs/heasarc/headates/how\\_many\\_xray.html](https://heasarc.gsfc.nasa.gov/docs/heasarc/headates/how_many_xray.html) The data for the number of VHE (TeV) gamma-ray sources is from TeVCat maintained by Deirdre Horan and Scott Wakely (retrieved 2017-09-28) : <http://tevcat.uchicago.edu/>

Go South!

(e.g., ALPACA [2022-24], Mega ALPACA, SWGO, CTA, ...) & Neutrinos





# Conclusions

- ✓ Tibet AS $\gamma$  experiment successfully observed UHE gamma rays from the Crab Nebula for the first time and opened new energy window. (Now >40 UHE  $\gamma$  ray sources detected by LHAASO, HAWC, H.E.S.S. and Tibet AS $\gamma$ )
- ✓ Tibet AS $\gamma$  experiment successfully observed Galactic diffuse gamma rays between 100 TeV and 1 PeV for the first time.
- ✓ Tibet UHE events (>400 TeV) do not originate from LHAASO UHE (>100 TeV) sources.
- ✓ IceCube diffuse neutrino flux smoothly connects to Tibet AS $\gamma$  diffuse gamma-ray flux assuming  $\pi^0$  best-fit model supporting the cosmic-ray origin.
- ✓ Tibet AS $\gamma$  experiment found a few PeVatron candidates associated with the molecular clouds.

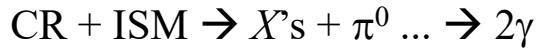
These facts indicate strong evidence that cosmic rays are accelerated beyond PeV energies in our Galaxy and spread over the Galactic disk.  
→ Search for more PeVatron candidates! → Go South!

Backup slides



# Composition Dependence

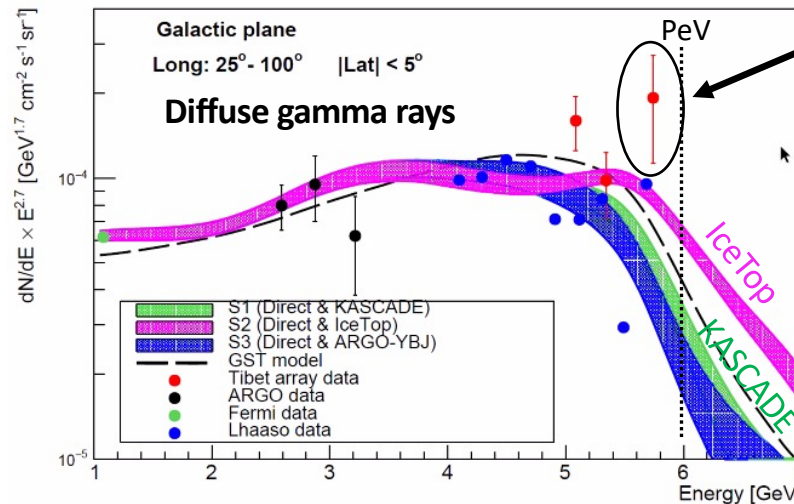
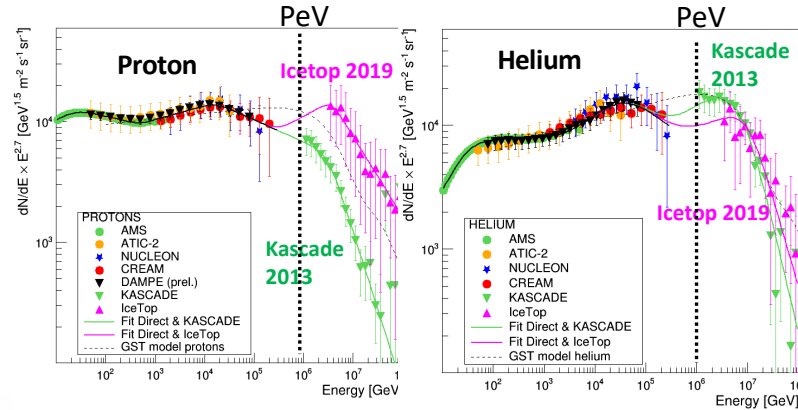
CRs interact with interstellar gas  
 ( $\gamma$ -ray energy has 10% of CRs)



→ Diffuse gamma-ray spectrum  
 depends on the CR composition

*Vernetto & Lipari (ICRC2021)*

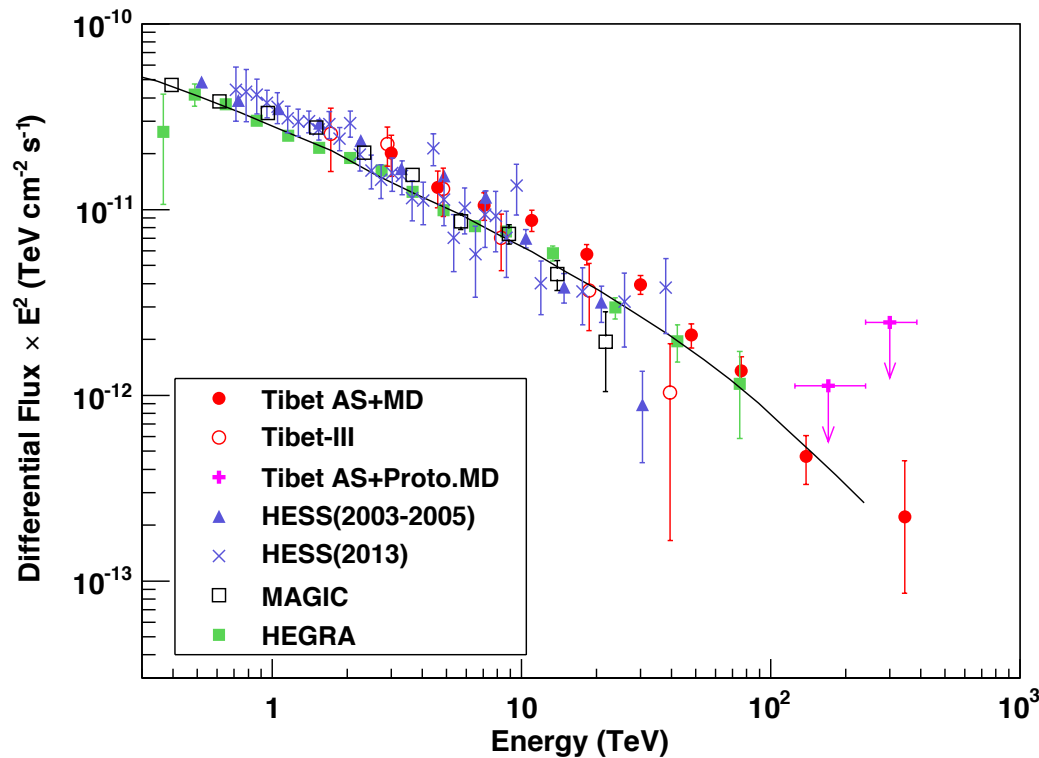
factor 1.5 – 2 difference@~600 TeV



4 ev / 10 ev from  
 Cygnus cocoon (< 4°)



# UHE $\gamma$ -rays from the Crab Nebula (2019)



*Amenomori+, PRL, 123, 051101, (2019)*

The highest energy  $\gamma \sim 450$  TeV

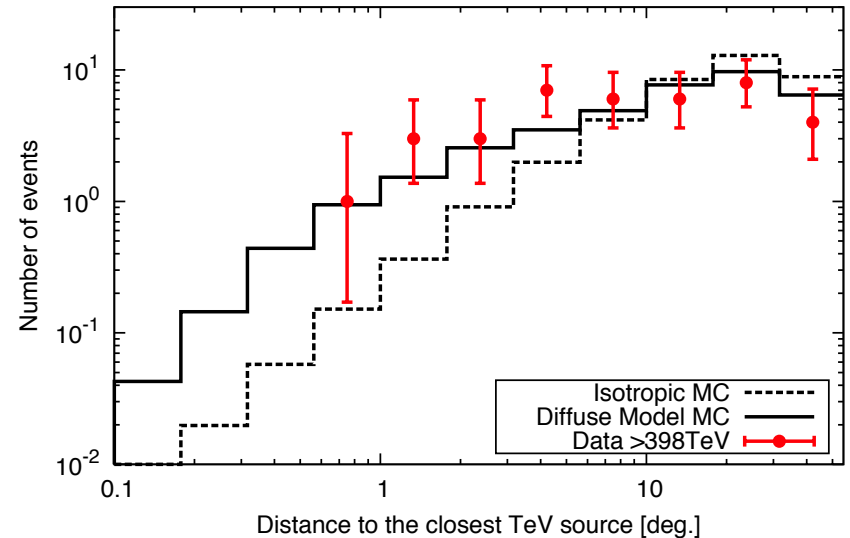
Thick curve :  
inverse Compton model  
normalized to HEGRA data  
*Aharonian+, ApJ, 614, 897 (2004)*



# Correlation with known TeV Sources

Correlation between UHE  $\gamma$ -rays above 398 TeV and 60 galactic sources from TeVCat catalog including UNID, PWN, Shell, Binary, SNR..., excluding GRB, HBL, IBL, LBL, BL Lac, AGN, Blazar, FSRQ, FRI, Starburst)

- ✓ No excess around known TeV sources
- ✓ Event distribution is consistent with diffuse model



- ✓ High-energy  $e^{+/-}$  lose their energy quickly.
- ✓ Cosmic-ray protons can escape farther from the source.



**Strong evidence for sub-PeV  $\gamma$  rays induced by cosmic rays**

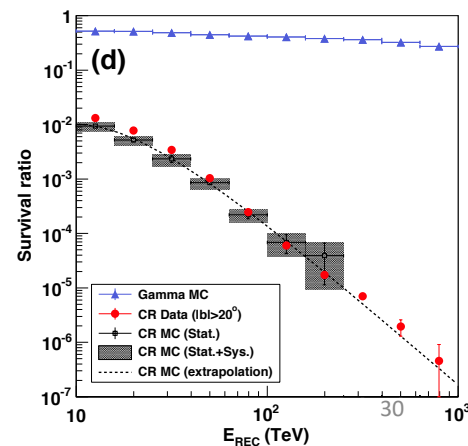
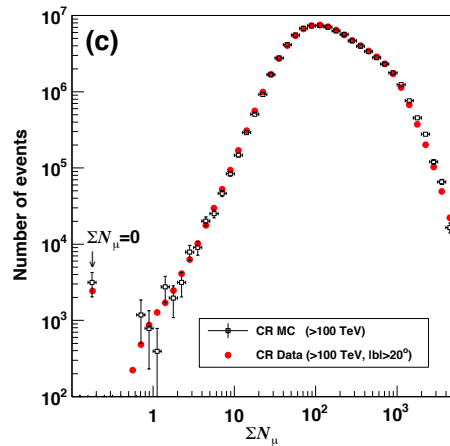
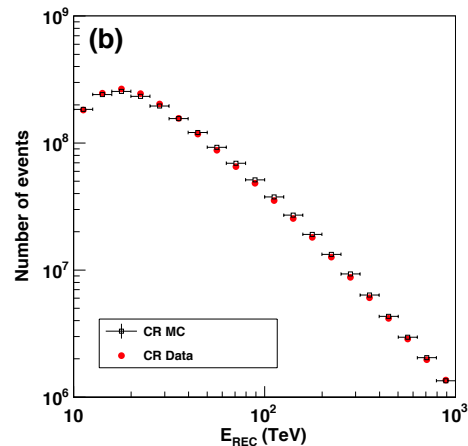
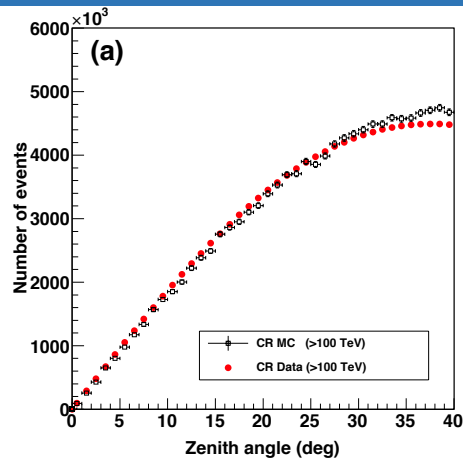


# Data/MC Comparison

- ✓ AS generation: CORSIKA
- ✓ Hadronic int. model:  
EPOS-LHC + FLUKA
- ✓ Detectors: GEANT4

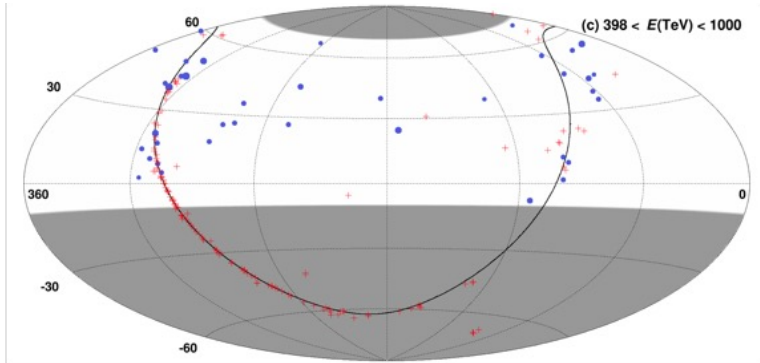
Reasonable agreement!

\*Note: Cosmic-ray MC simulation is not used for the flux calculation or for any optimization of the analysis.





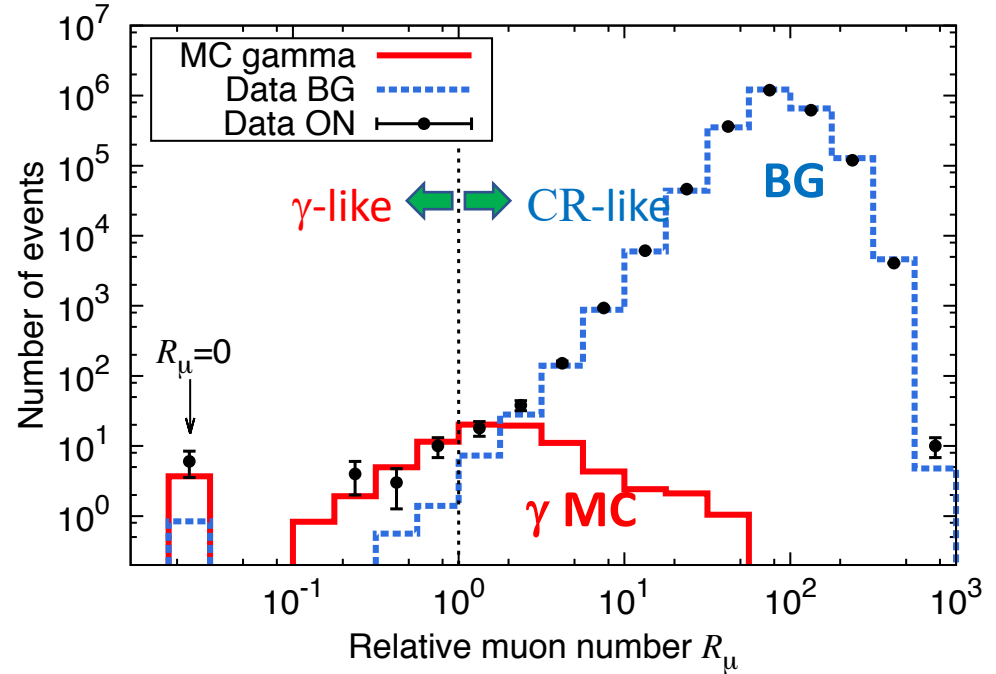
# Muon Number Distribution (>398 TeV)



- ON region  $|b| < 10^\circ$
- ⋯ BG region  $|b| > 20^\circ$

Gamma Survival ratio :  
30% by MC sim (>398TeV)

CR Survival ratio :  
 $\sim 10^{-6}$  (>398TeV= $10^{2.6}$ TeV)



$$R_\mu = \frac{\text{Observed \# of muons}}{\text{\# of muons at the cut value}}$$



# Data Table

TABLE S1. Number of events observed by the Tibet AS+MD array in the direction of the galactic plane. The galactic longitude of the arrival direction is integrated across our field of view (approximately  $22^\circ < l < 225^\circ$ ). The ratios ( $\alpha$ ) of exposures between the ON and OFF regions are 0.135 for  $|b| < 5^\circ$  and 0.27 for  $|b| < 10^\circ$ , respectively.

| Energy bin<br>(TeV) | $N_{\text{ON}}$ | $ b  < 5^\circ$                                  |                              | $ b  < 10^\circ$ |  |                              |
|---------------------|-----------------|--|------------------------------|------------------|--|------------------------------|
|                     |                 | $N_{\text{BG}}$<br>( $= \alpha N_{\text{OFF}}$ ) | Significance<br>( $\sigma$ ) | $N_{\text{ON}}$  | $N_{\text{BG}}$<br>( $= \alpha N_{\text{OFF}}$ ) | Significance<br>( $\sigma$ ) |
| 100 – 158           | 513             | 333  | 8.5                          | 858              | 655  | 6.6                          |
| 158 – 398           | 117             | 58.1   | 6.3                          | 182              | 114  | 5.1                          |
| 398 – 1000          | 16              | 1.35   | 6.0                          | 23               | 2.73   | 5.9                          |

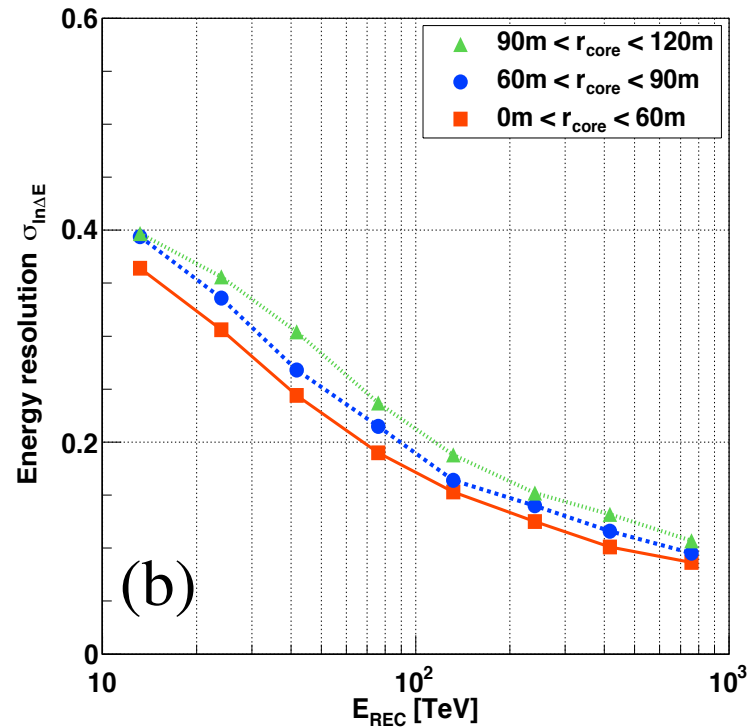
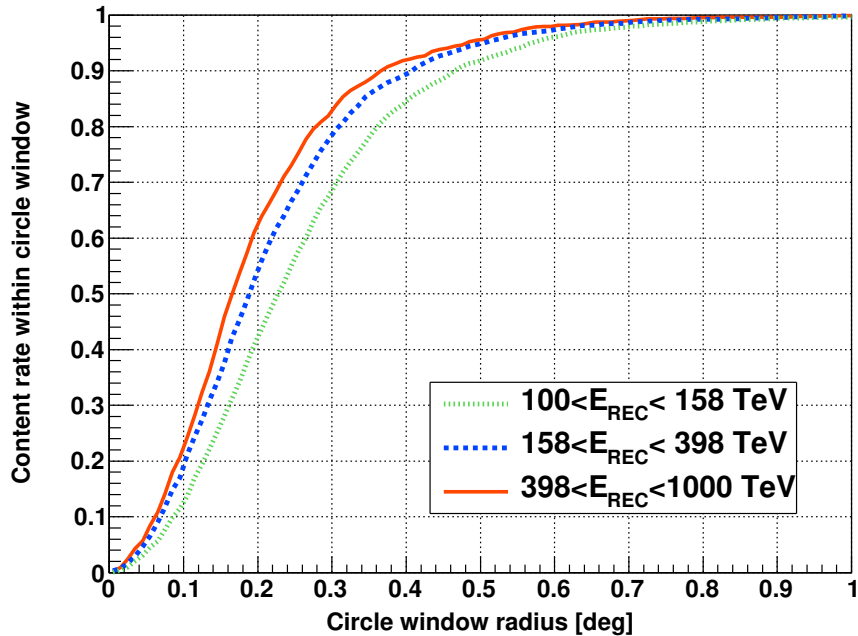
TABLE S2. Galactic diffuse gamma-ray fluxes measured by the Tibet AS+MD array.

| Energy bin<br>(TeV) | Representative $E$<br>(TeV) | Flux ( $25^\circ < l < 100^\circ,  b  < 5^\circ$ )<br>( $\text{TeV}^{-1} \text{ cm}^{-2} \text{ s}^{-1} \text{ sr}^{-1}$ ) |  | Flux ( $50^\circ < l < 200^\circ,  b  < 5^\circ$ )<br>( $\text{TeV}^{-1} \text{ cm}^{-2} \text{ s}^{-1} \text{ sr}^{-1}$ ) |  |
|---------------------|-----------------------------|--|--|--|--|
|                     |                             |  |  |  |  |
| 100 – 158           | 121                         | $(3.16 \pm 0.64) \times 10^{-15}$  |  | $(1.69 \pm 0.41) \times 10^{-15}$  |  |
| 158 – 398           | 220                         | $(3.88 \pm 1.00) \times 10^{-16}$  |  | $(2.27 \pm 0.60) \times 10^{-16}$  |  |
| 398 – 1000          | 534                         | $(6.86^{+3.30}_{-2.40}) \times 10^{-17}$   |  | $(2.99^{+1.40}_{-1.02}) \times 10^{-17}$   |  |





# Angular/Energy Resolutions





# CASA-MIA Observation

TABLE 1  
LIMITS TO DIFFUSE EMISSION

| Region<br>( $50^\circ < l < 200^\circ$ ) | Median<br>Energy<br>(TeV) | Significance<br>( $\sigma$ ) | $J_\gamma/J_{CR}$ 90% C.L.<br>( $10^{-5}$ ) |
|--|---------------------------|------------------------------|---|
| $-2^\circ < b < 2^\circ$ .....           | 140                       | +1.78                        | 7.2   |
|  | 180                       | +1.81                        | 3.8   |
|  | 310                       | +2.56                        | 5.2   |
|  | 650                       | +1.12                        | 3.2   |
|  | 1300                      | +0.07                        | 4.6   |
| $-5^\circ < b < 5^\circ$ .....           | 140                       | +1.63                        | 3.4   |
|  | 180                       | +0.08                        | 2.6   |
|  | 310                       | +0.86                        | 2.4   |
|  | 650                       | +1.60                        | 2.6   |
|  | 1300                      | +0.06                        | 3.5   |
| $-10^\circ < b < 10^\circ$ .....         | 140                       | +2.39                        | 2.8   |
|  | 180                       | +1.79                        | 2.2   |
|  | 310                       | +0.87                        | 2.3   |
|  | 650                       | +0.91                        | 1.8   |
|  | 1300                      | -0.56                        | 2.3   |

NOTE.—Tabulated upper limits to diffuse gamma-ray emission from the plane of the Galaxy. Although positive excesses are seen, we do not view these as statistically significant enough to claim detections. Flux limits are tabulated for bands along the Galactic plane from  $|b| < 2^\circ$  to  $|b| < 10^\circ$ . Median energy is quoted for integral flux limits. Selected spatial regions and energy bands are not statistically independent.

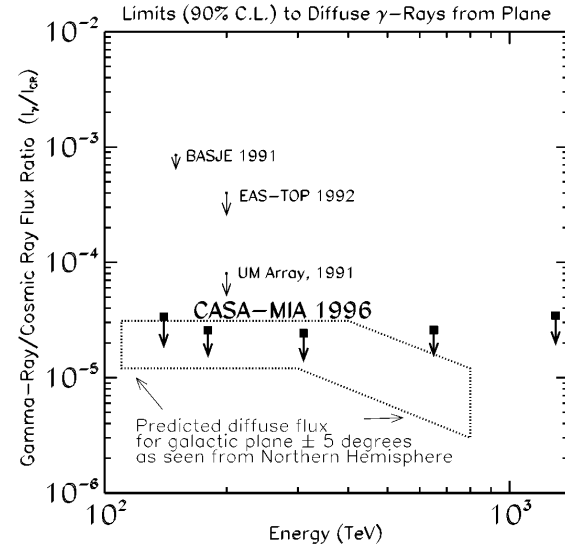


FIG. 4.—CASA-MIA sensitivity to diffuse gamma-ray emission from the central plane of the Galaxy ( $|b| < \pm 5^\circ$ ,  $50^\circ < l < 200^\circ$ ). Sensitivities are given in terms of the fraction of gamma rays relative to the detected all-particle flux of cosmic rays at the Earth. Also shown are limits from previous experiments (BASJE—Kakimoto et al. 1991; EAS-TOP—Aglietta et al. 1992, UM—Matthews et al. 1991). Predicted flux from Aharonian (1991).

*Borione et al., Astrophys. J. 493, 175 (1998)*

$$[I_\gamma] / [I_{CR}] \sim 3 \times 10^{-5}$$

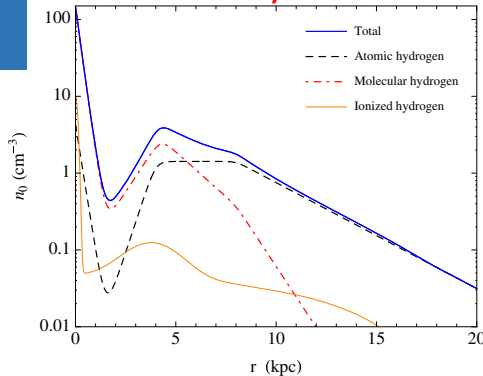


# Diffuse Model

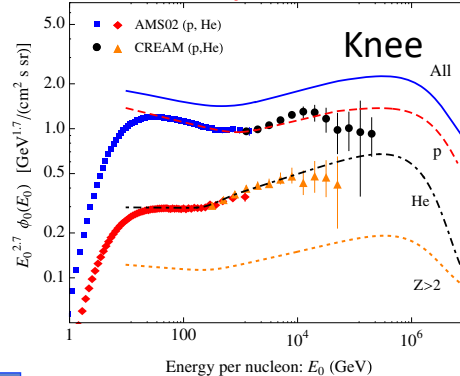
*Lipari & Vernetto, PRD (2018)*

Model can reproduce global structure  
(not considered of the local structures)

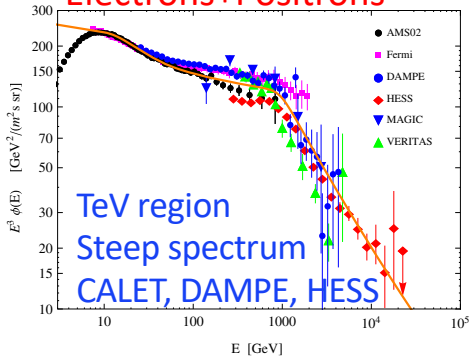
## Gas density



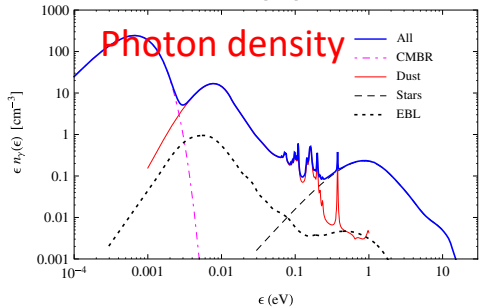
## Cosmic rays



## Electrons+Positrons



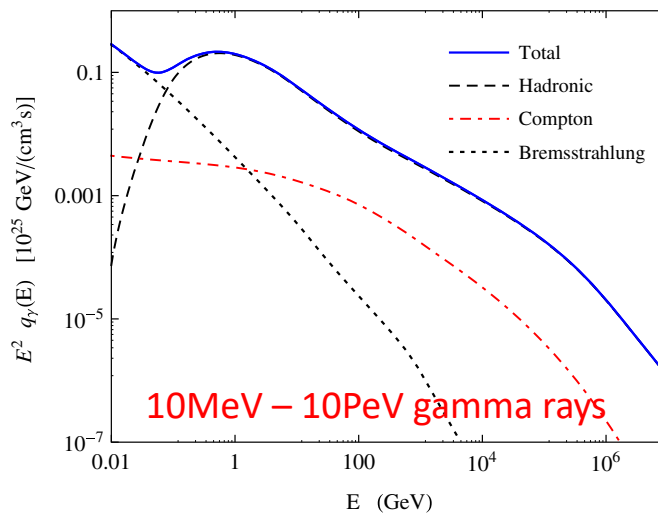
## Photon density



Brems.

Hadronic

Compton





# Cosmic Ray Pool × ISM

High-energy  
cosmic rays

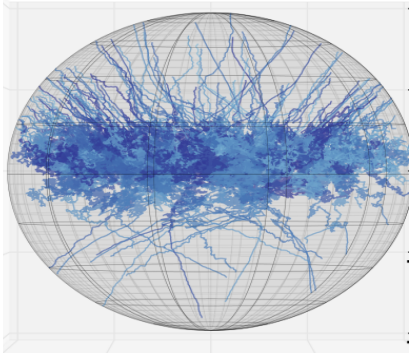
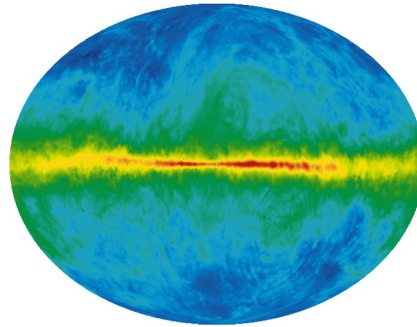


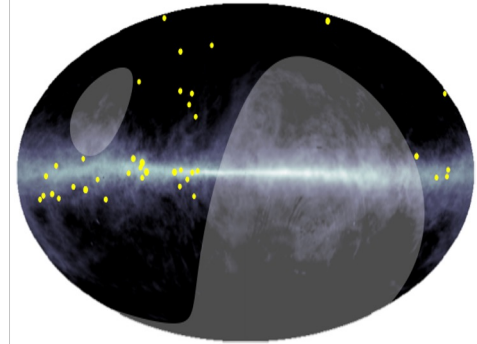
Figure from slide presented by A. Kääpä (Bergische Universität Wuppertal) at CRA2019 workshop

Interstellar  
matter



Radio (21cm) HI Map  
Hartmann et al. (1997)  
Dickey & Lockman (1990)

High-energy  
gamma rays



**This Work**

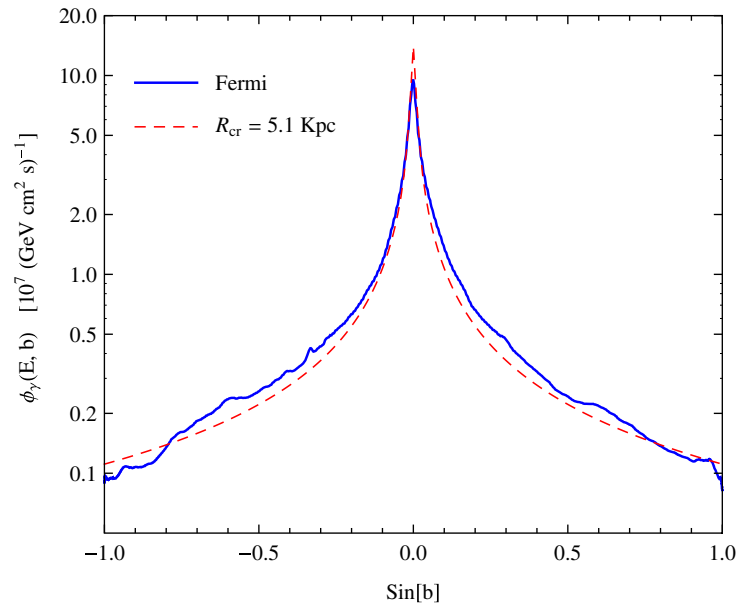
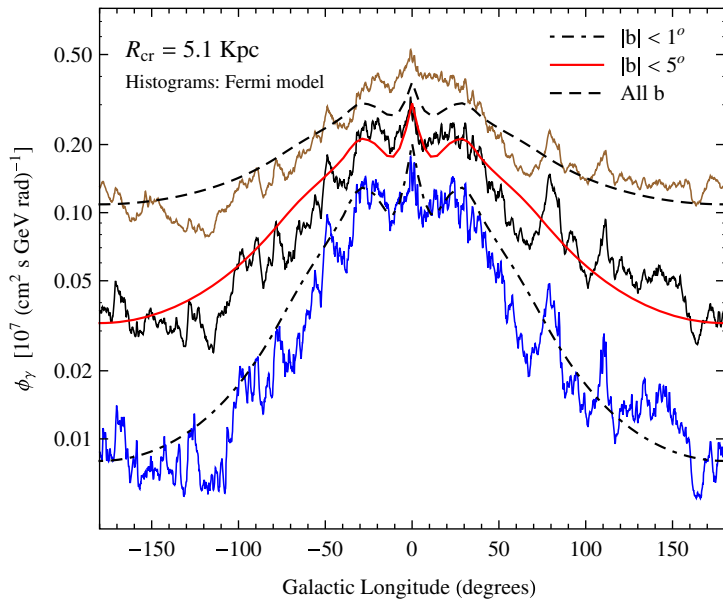
✓ This work proves a theoretical model that cosmic rays produced by PeVatrons are trapped in the Galactic magnetic field for millions of years, forming a pool of cosmic rays.



# Reproducing Fermi-LAT Results

Model can reproduce global structure  
(not taken into account of local structure)

*Lipari & Vernetto, PRD (2018)*

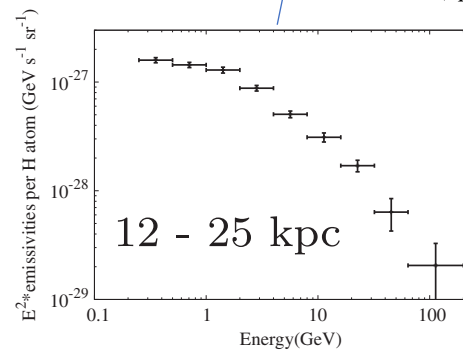
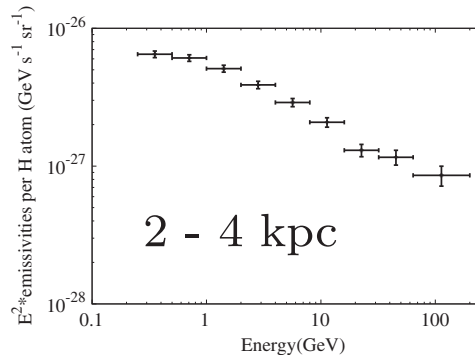
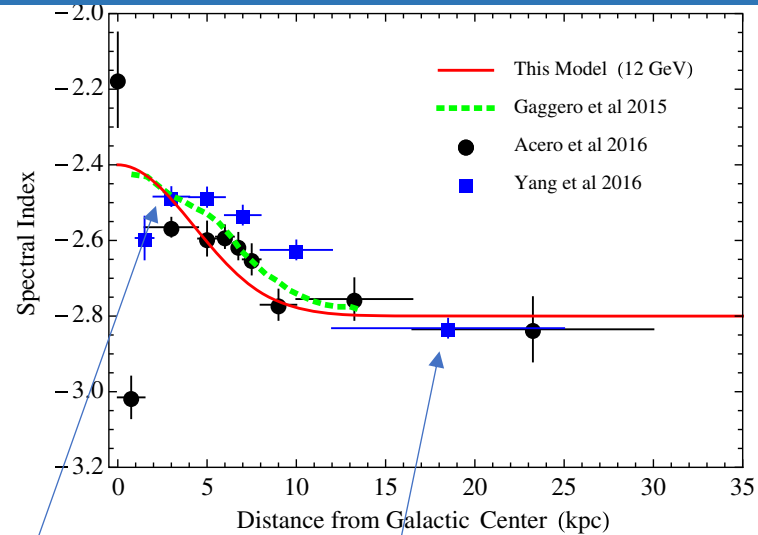




# Space Dependence of CR Spectrum

*Lipari & Vernetto, PRD (2018)*

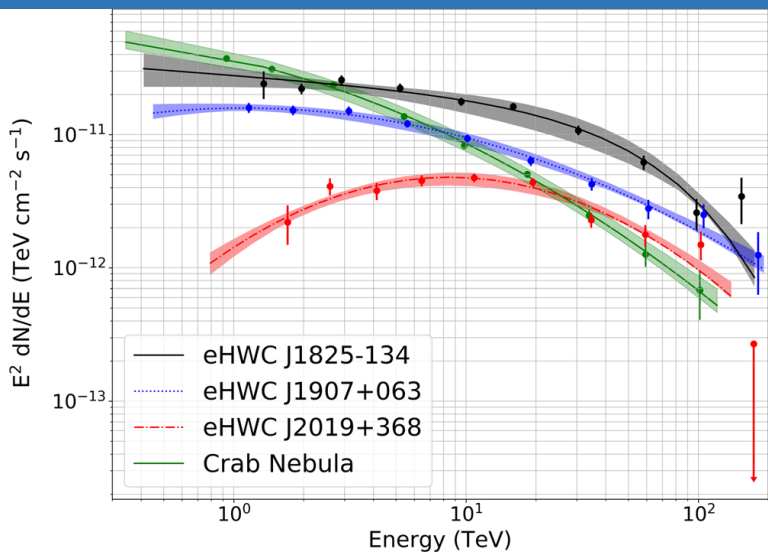
Harder gamma-ray spectral index,  
getting closer to the G.C. @12 GeV



*Yang et al., Phys. Rev. D 93, 123007 (2016)*



# How to Identify PeVatrons



eHWC J1825-134 (PWN?)

- PSR J1826-1334
- PSR J1826-1256
- A few SNRs ...

eHWC J1907+063 (PWN?)

- PSR J1907+0602
- SNR G40.5-0.5

eHWC J2019+368 (PWN?)

- ✓ Hard spectral index ( $\sim -2$ )
- ✓ Extended morphology



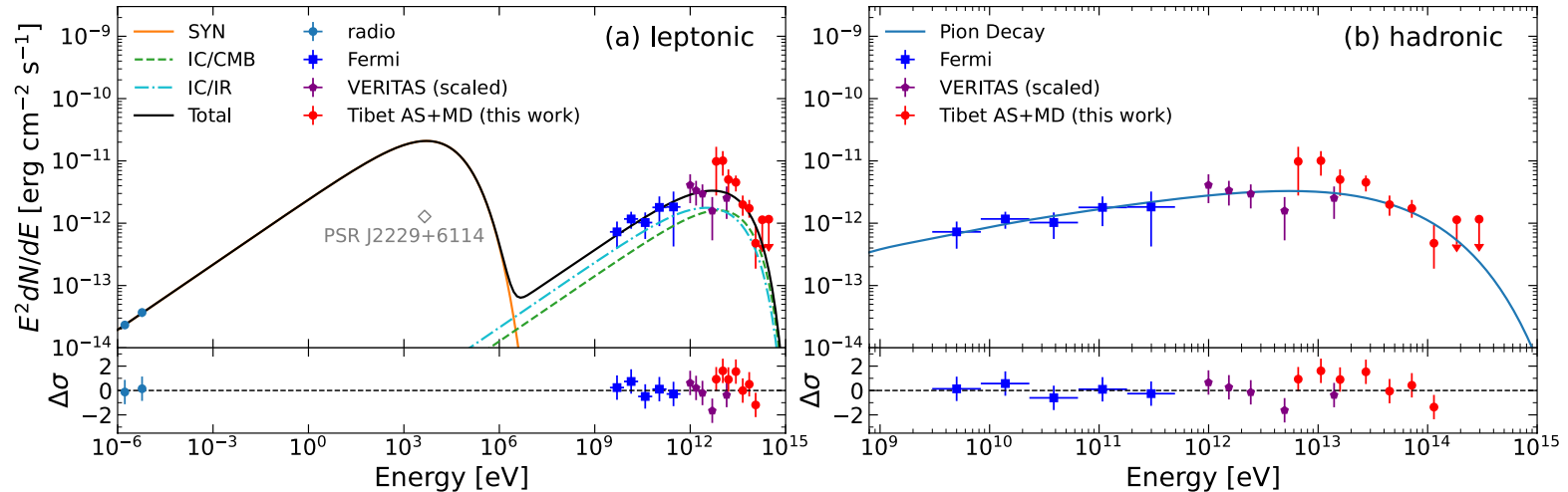
| Source name      | RA (°)        | Dec (°)       | Extension > 56 TeV (°) | $F$ ( $10^{-14}$ ph cm $^{-2}$ s $^{-1}$ ) | $\sqrt{TS}$ > 56 TeV | Nearest 2HWC source | Distance to 2HWC source(°) | $\sqrt{TS}$ > 100 TeV |
|------------------|---------------|---------------|------------------------|--|----------------------|---------------------|----------------------------|-----------------------|
| eHWC J0534 + 220 | 83.61 ± 0.02  | 22.00 ± 0.03  | PS                     | 1.2 ± 0.2                                  | 12.0                 | J0534 + 220         | 0.02                       | 4.44                  |
| eHWC J1809 - 193 | 272.46 ± 0.13 | -19.34 ± 0.14 | 0.34 ± 0.13            | 2.4 $^{+0.6}_{-0.5}$                       | 6.97                 | J1809 - 190         | 0.30                       | 4.82                  |
| eHWC J1825 - 134 | 276.40 ± 0.06 | -13.37 ± 0.06 | 0.36 ± 0.05            | 4.6 ± 0.5                                  | 14.5                 | J1825 - 134         | 0.07                       | 7.33                  |
| eHWC J1839 - 057 | 279.77 ± 0.12 | -5.71 ± 0.10  | 0.34 ± 0.08            | 1.5 ± 0.3                                  | 7.03                 | J1837 - 065         | 0.96                       | 3.06                  |
| eHWC J1842 - 035 | 280.72 ± 0.15 | -3.51 ± 0.11  | 0.39 ± 0.09            | 1.5 ± 0.3                                  | 6.63                 | J1844 - 032         | 0.44                       | 2.70                  |
| eHWC J1850 + 001 | 282.59 ± 0.21 | 0.14 ± 0.12   | 0.37 ± 0.16            | 1.1 $^{+0.3}_{-0.2}$                       | 5.31                 | J1849 + 001         | 0.20                       | 3.04                  |
| eHWC J1907 + 063 | 286.91 ± 0.10 | 6.32 ± 0.09   | 0.52 ± 0.09            | 2.8 ± 0.4                                  | 10.4                 | J1908 + 063         | 0.16                       | 7.30                  |
| eHWC J2019 + 368 | 304.95 ± 0.07 | 36.78 ± 0.04  | 0.20 ± 0.05            | 1.6 $^{+0.3}_{-0.2}$                       | 10.2                 | J2019 + 367         | 0.02                       | 4.85                  |
| eHWC J2030 + 412 | 307.74 ± 0.09 | 41.23 ± 0.07  | 0.18 ± 0.06            | 0.9 ± 0.2                                  | 6.43                 | J2031 + 415         | 0.34                       | 3.07                  |

*Abeysekara et al., PRL, 124, 021102 (2020)*



# PeVatron Candidate: SNR G106.3+2.7

*Amenomori et al., Nat. Astron (2021)*



Electron spectrum:  $\alpha=-2.3$ ,  $E_{\text{cut}}=190\text{TeV}$

Magnetic field:  $B=8.6\mu\text{G}$

→ Cooling time  $\tau_{\text{sync}}=0.9\text{kyr} \ll \text{SNR age } 10\text{kyr}$

The required total energy of electrons is  $\sim 1.4 \times 10^{47}$  erg, which only takes up  $\sim 2\%$  of the spin-down energy released in the entire pulsar lifetime. If the rest of the spin-down energy goes into the magnetic field, the average magnetic field in the PWN would be much larger than the required value of  $8 \mu\text{G}$  and results in very large fluxes at radio and X-ray wavelengths.





# Pulsar Halo Model of Diffuse $\gamma$ -Rays

Tim Linden and Benjamin J. Buckman, *PHYSICAL REVIEW LETTERS* 120, 121101 (2018)

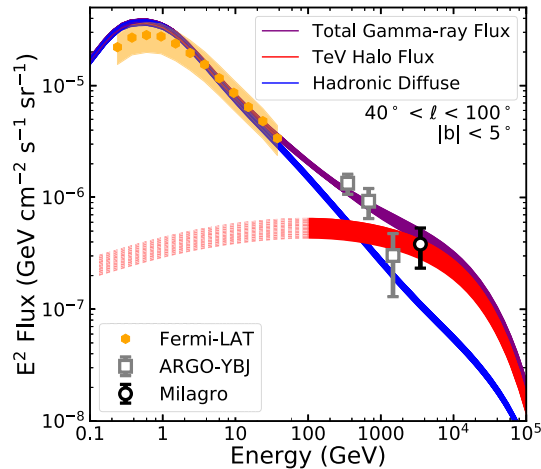


FIG. 1. The contribution of subthreshold TeV halos to the diffuse  $\gamma$ -ray emission along the galactic plane in the region  $40^\circ < \ell < 100^\circ$ , and  $|b| < 5^\circ$ , compared to observations by the Fermi-LAT (described in the text), ARGO-YBJ [5], and Milagro [1]. The background (blue) corresponds to the predictions of 128 GALPROP models of diffuse  $\gamma$ -ray emission [8]. The contribution from TeV halos (red) is described in the text. TeV halos naturally reproduce the TeV excess observed by Milagro, while remaining consistent with ARGO-YBJ observations. The dashed red region indicates our ignorance of low-energy  $\gamma$ -ray emission from TeV halos.

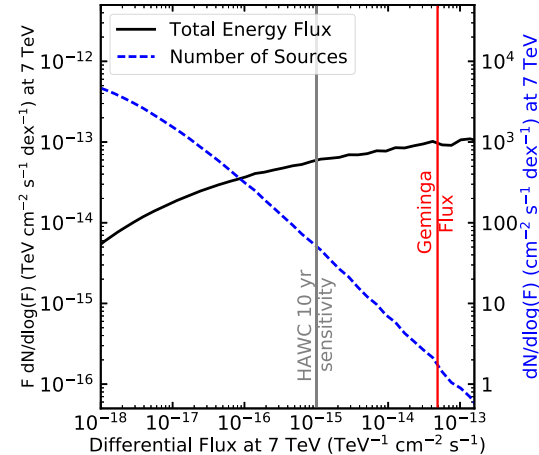
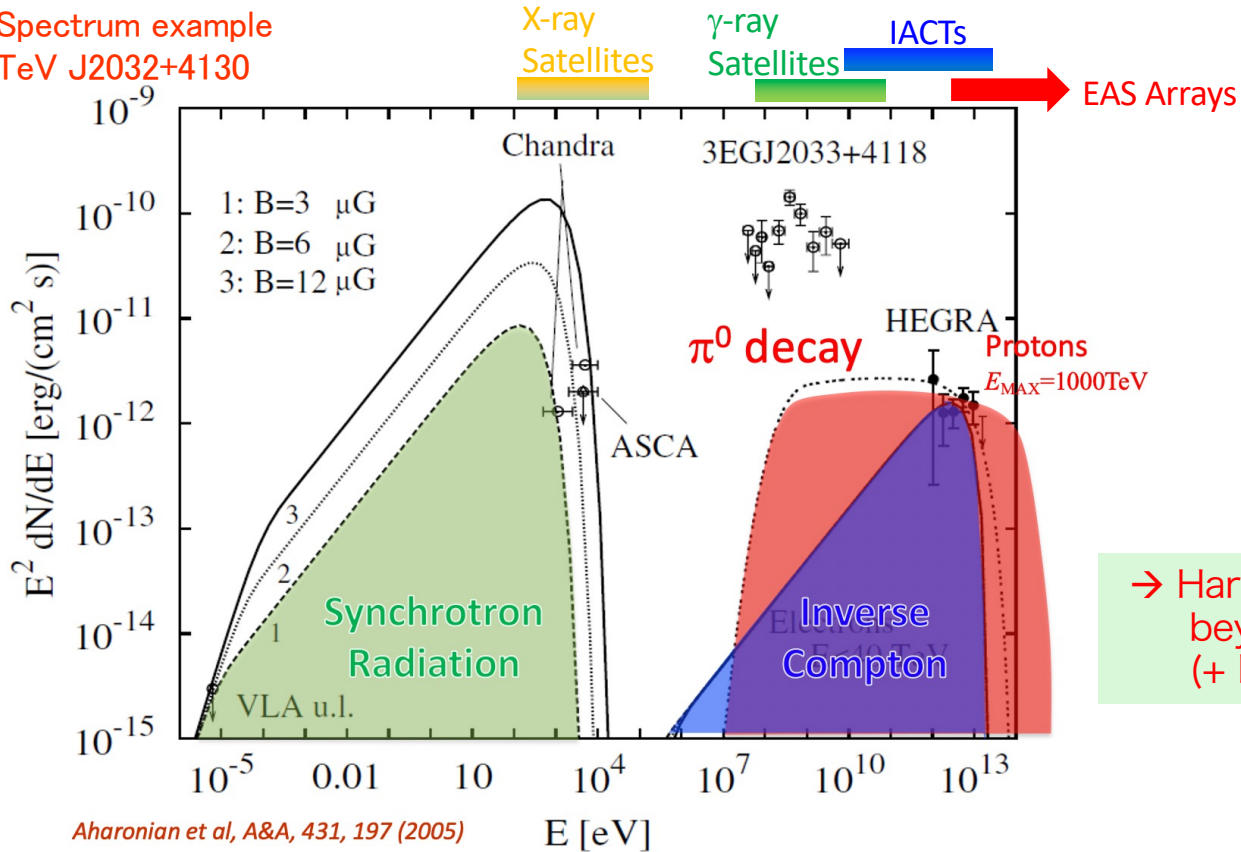


FIG. 3. The contribution of individual TeV halos to the TeV excess in the region  $40^\circ < \ell < 100^\circ$ , and  $|b| < 5^\circ$ . We normalize our results at 7 TeV [19], assuming that individual TeV halos convert their spin-down luminosity into 7 TeV  $\gamma$  rays with an identical efficiency as Geminga. Vertical lines correspond to the flux of Geminga, and the projected 10 yr HAWC sensitivity. Results are shown for the total  $\gamma$ -ray flux [ $F dN/d\log_{10}(F)$ , black, left y axis], which indicates that most of the  $\gamma$ -ray intensity stems from the bright TeV halos, as well as for the source count [ $dN/d\log_{10}(F)$ , blue, right y axis], which indicates that 10 yr HAWC data will observe  $\sim 50$  TeV halos in the ROI. For illustrative purposes, in this plot we show the contribution from TeV halos with individual fluxes exceeding Geminga, predicting the existence of only  $\sim 1$  such system.



# How to Identify PeVatrons

Spectrum example  
TeV J2032+4130



Aharonian et al, A&A, 431, 197 (2005)



# How to Identify PeVatrons

- $\gamma$ -ray beyond 100 TeV by Tibet, HAWC etc. in North, ALPACA, SWGO in south will come soon
- Spectral index  $\alpha \sim -2$  in TeV by IACTs
- Coincident with molecular cloud observed by radio
- $\pi^0$  cutoff around 70 MeV by  $\gamma$ -ray satellites
- Dark in X-ray observation
- Deep observation by IACTs to resolve sources
- Coincident with HE neutrino by IceCube

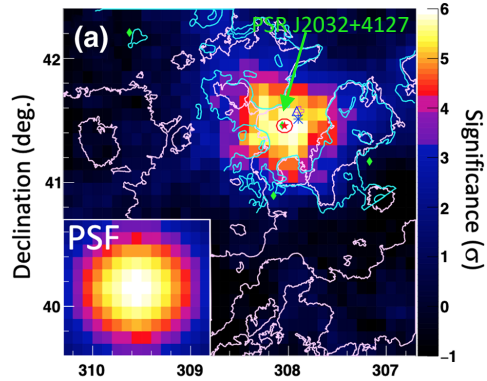
**Multi-wavelength Multi-particle Observations**



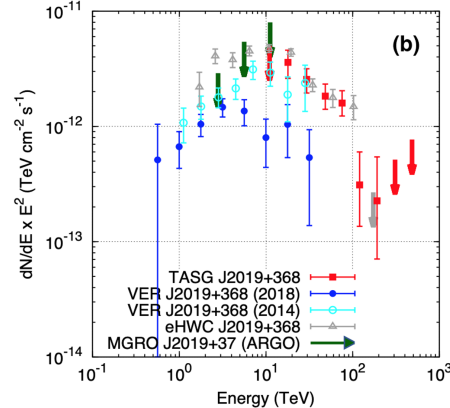
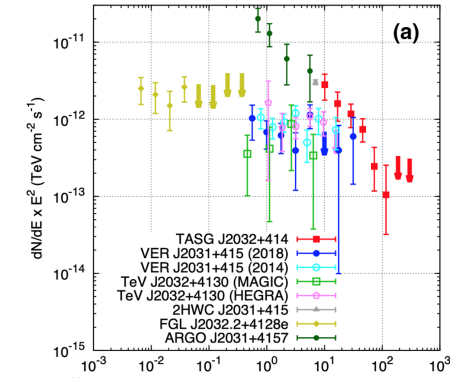
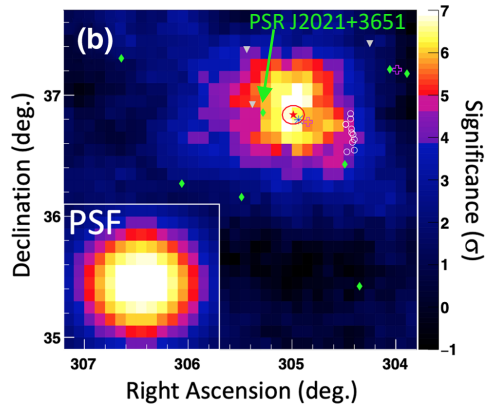
# Cygnus OB1 & OB2 in the 100 TeV region

*Amenomori et al., PRL, 127, 031102 (2021)*

Cyg. OB2

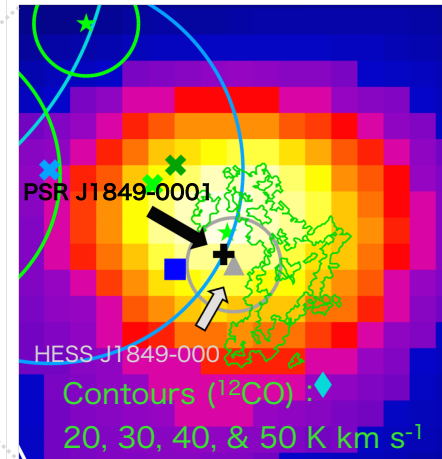
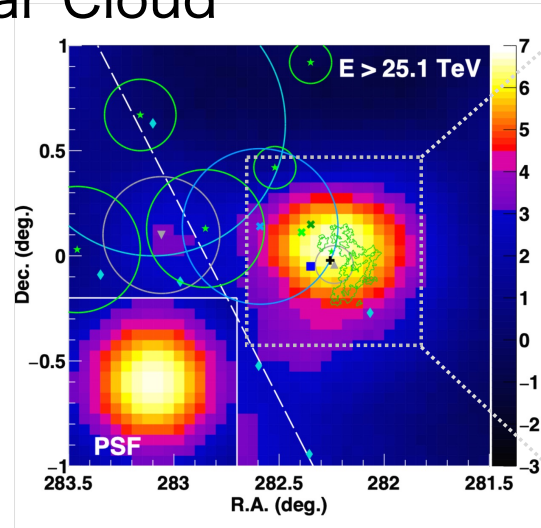
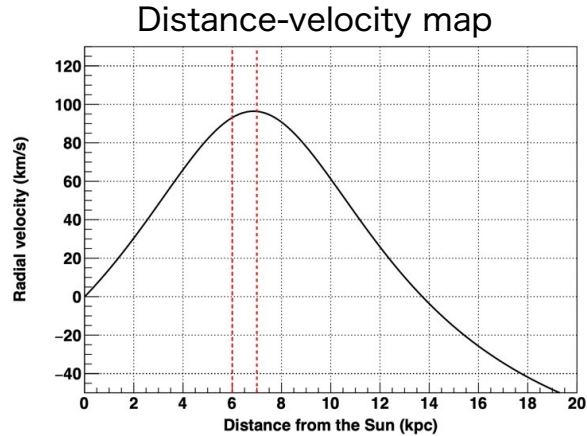


Cyg. OB1





## Detection of a Molecular Cloud



✓ Analysis of archive  $^{12}\text{CO}$  (J=1-0) data (FUGIN<sup>1</sup>)

✓ Assumed istance : 7 kpc<sup>2</sup>

✓ Integration of velocity range of 93-100 km s<sup>-1</sup>

=> A ~20 pc size cloud w/  $T_b$  ~20 K km s<sup>-1</sup> @ the west of HESS J1849-000

✓ Overlap b/w  $\gamma$ -ray emission & cloud

✓ Gas density :  $n_p = X_{\text{co}} T_{\text{mb}} / R \sim 70 \text{ cm}^{-3}$  ( $X_{\text{co}} = 2 \times 10^{20} \text{ cm}^{-2} (\text{K km s}^{-1})^{-1}$ )<sup>3</sup>

=> Can provide the gas density of  $\geq$  10 cm<sup>-3</sup>

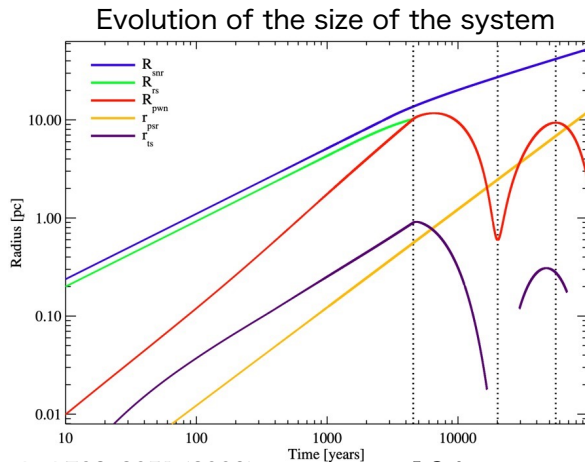
1. Umemoto+, PASJ 69, 5 (2017)
2. Gotthelf+, ApJL 729, L16 (2011)
3. Bolatto+, Ann. Rev. Astron. Astrophys 51, 207 (2013)



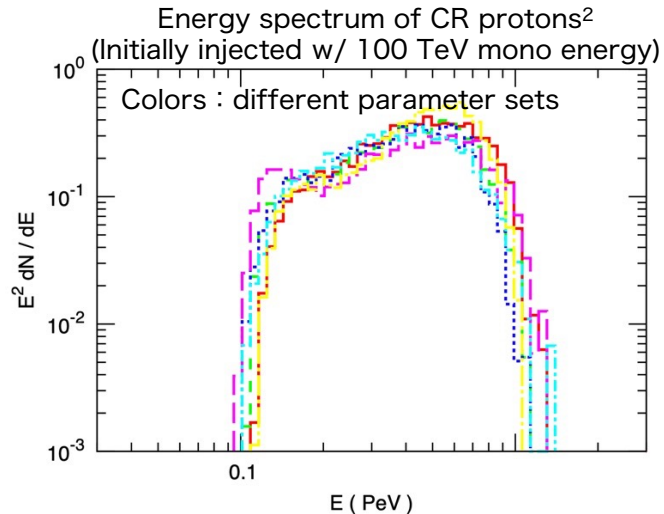
# Adiabatic Compression for HESS J1849-000

## Possible Acceleration Mechanism of PeV CRs

- ✓ CR acceleration in a **PWN-SNR composite system**<sup>1,2</sup> ??
    - CR protons pre-accelerated up to  $\sim 100$  TeV in the SNR FS are re-accelerated up to  $\sim 1$  PeV in the PWN compressed by the SNR reverse shock
    - $\sim 10^{49}$  erg is given to the accelerated particles<sup>1</sup>
    - PWN is compressed to  $\sim 10\%$  of the original size<sup>1,2</sup>
    - $B$  of the PWN is amplified up to  $\sim 100 \mu\text{G}$ <sup>1</sup>
- => compact synchrotron X-ray emission by  $e^\pm$  of PWN origin??



10 kyr



1. Gelfand+, ApJ 703, 2051 (2009)  
2. Ohira+, MNRAS 478, 926 (2018)



# TASG J1844-038

## Discussion (1): Association of TASG J1844-038 w/ SNR G28.6-0.1 (1)

### SNR G28.6-0.1

- Nonthermal radio<sup>1)</sup> & X-rays<sup>2)</sup> by electron synchrotron radiation
- Shell-type SNR<sup>2)</sup>
- Distance:  $9.6 \pm 0.3$  kpc<sup>3)</sup>
- Age: 2.7 kyr<sup>2)</sup> or 19 kyr<sup>3)</sup>

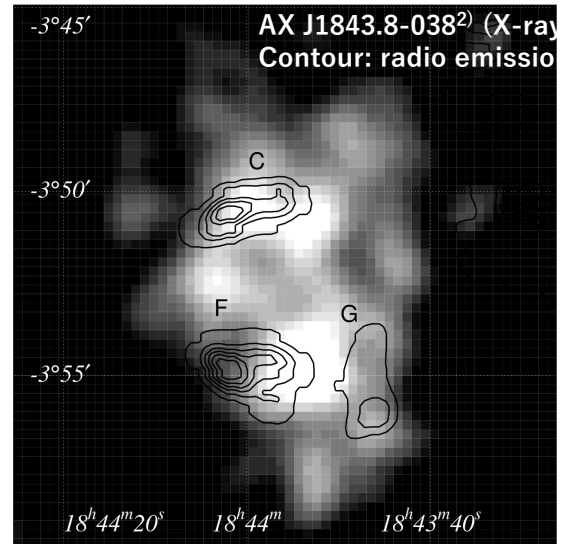
TASG J1844-038's radius:  $\sigma = 0.34^\circ \pm 0.12^\circ$

AX J1843.8-0352's radius (X-rays):  $\sigma_{\text{mean}} = 0.075^\circ (4.5')^4$

Discrepancy in their extensions at the  $2.3 \sigma$  level

=> Contribution of gamma rays of hadronic origin ?  
(CR interaction w/ ambient molecular clouds ?)

- 1) Helfand et al., ApJ 341, 151 (1989)
- 2) Bamba et al., PASJ 53, L21 (2001)
- 3) Ranasinghe & Leahy, MNRAS 477, 2243 (2018)
- 4) Ueno et al., ApJ 588, 338 (2003)

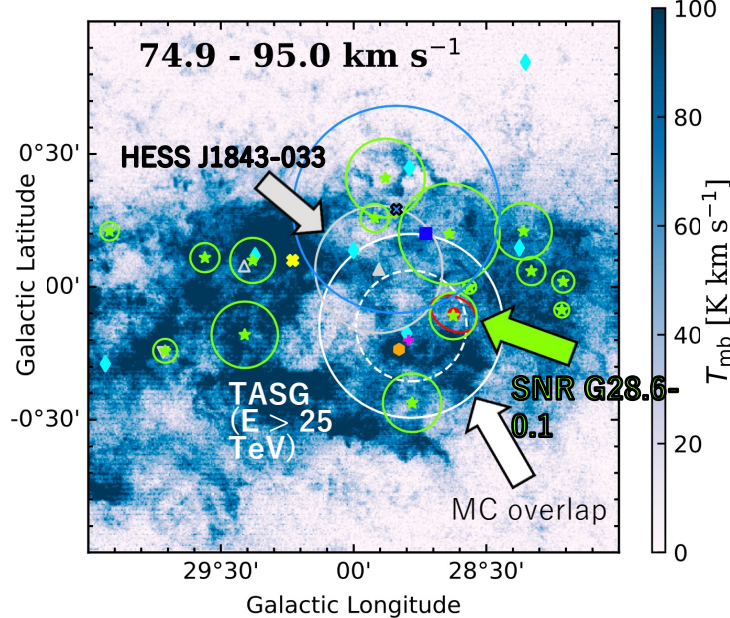




# TASG J1844-038

## Discussion (1): Association of TASG J1844-038 w/ SNR G28.6-0.1 (2)

$^{12}\text{CO}$  ( $J = 1 - 0$ ) map from the FUGIN data<sup>1)</sup>



Several resemblances to **SNR G106.3+2.72**):

1. Overlapping molecular clouds (MCs),
2. Max. energy of CR protons:  $\approx 500\text{TeV}$ , &
3. Average of the estimated ages is  $\approx 10$  kyr.

=> **Could have been a PeVatron in the past??**

Diffusion time of CR protons through MCs<sup>3)</sup>:

$$\tau_{\text{diff}} = \frac{R_{\text{cl}}^2}{6D(E)} \sim 1.2 \cdot 10^4 \chi^{-1} \left( \frac{R_{\text{tot}}}{20 \text{ pc}} \right)^2 \left( \frac{E}{\text{GeV}} \right)^{-0.5} \left( \frac{B}{10 \mu\text{G}} \right)^{0.5} \text{ yr}$$

where  $R$ , size of MCs &  $\chi$ , suppression factor.

Assuming  $\chi = 0.1$  &  $B = 10 \mu\text{G}$  ( $n_{\text{H}} \sim 100 \text{ cm}^{-3}$ ),

$$\tau_{\text{diff}}(R_{\text{TASG}}, E_{\text{CR}} > 250 \text{ TeV}) \lesssim 2.0 \text{ kyr} \ \&$$

$$\tau_{\text{diff}}(R_{\text{HESS}}, E_{\text{CR}} \approx 10 \text{ TeV}) \approx 4.9 \text{ kyr}.$$

Acceptable compared w/ the SNR's age

- 1) Umemoto et al., PASJ 69, 78 (2017)
- 2) Amenomori et al., Nat. Astron. 5, 460 (2021)
- 3) Gabici et al., Astrophys. Space Sci. 309, 365 (2007)

Amenomori et al., *ApJ* 932, 120 (2022)





# TASG J1844-038

## Discussion (2): Association of TASG J1844-038 w/ PSR J1844-0346 PSR J1844-0346

- Gamma-ray PSR discovered by the Einstein@home project<sup>1)</sup>
- $P = 113$  ms,  $\tau_c = 12$  kyr &  $\dot{E} = 4.2 \times 10^{36}$  erg s<sup>-1</sup>
- Pseudo distance: 4.3 kpc<sup>2)</sup>

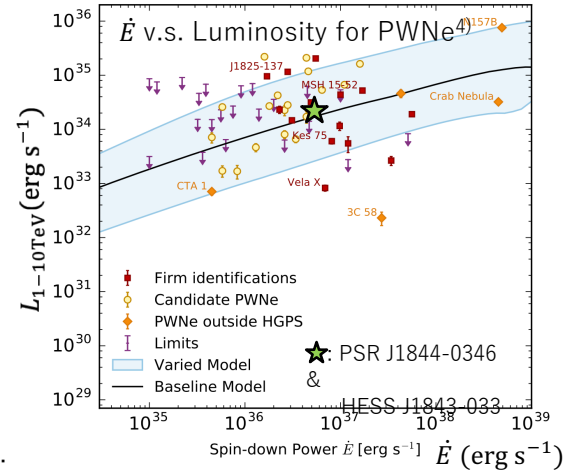
### HESS J1843-033<sup>3)</sup>

- $L(1 \text{ TeV} < E < 10 \text{ TeV}) = 2.4 \times 10^{34}$  erg s<sup>-1</sup> <sup>3)</sup> (@ 4.3 kpc)
- Size:  $\approx 18$  pc (@ 4.3 kpc)
- Spectral index:  $\approx 2.0$  (from the ECPL fit in this work)

=> has characteristics typical of TeV PWNe<sup>4)</sup>.

### ICS off CMB is acceptable

- $e^\pm$  w/  $E \approx 90$  TeV scatters off CMB up to  $E_{\gamma, \text{cutoff}} \approx 50$  TeV<sup>5)</sup>.
- Size of TASG J1844-038:  $\approx 26$  pc (@ 4.3 kpc)
- Assuming Geminga-like env.<sup>6)</sup> with  $B = 3 \mu\text{G}$ ,  $D = 4.4 \times 10^{27}$  cm<sup>2</sup> s<sup>-1</sup>,  
 $\tau_{\text{diff}} \approx 8$  kyr
- Cooling time of  $e^\pm$  by sync. & ISC<sup>5)</sup>:  $\tau_{\text{cool}} \approx 11$  kyr  
 =>  $\tau_{\text{diff}} < \tau_{\text{cool}}$  &  $\tau_{\text{diff}} < \tau_c$

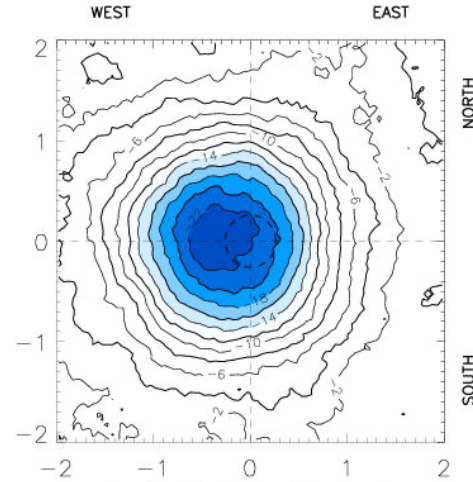


- 1) Clark et al., ApJ 834, 106 (2017)
- 2) Devin et al., A&A 647, 68 (2021)
- 3) H.E.S.S. collaboration, A&A 612, A1 (2018)
- 4) H.E.S.S. collaboration, A&A 612, A2 (2018)
- 5) Hinton & Hofmann, Ann. Rev. of Astron. & Astrophys. 47, 523 (2009)
- 6) Abeyssekara et al., Science 358, 911 (2017b)

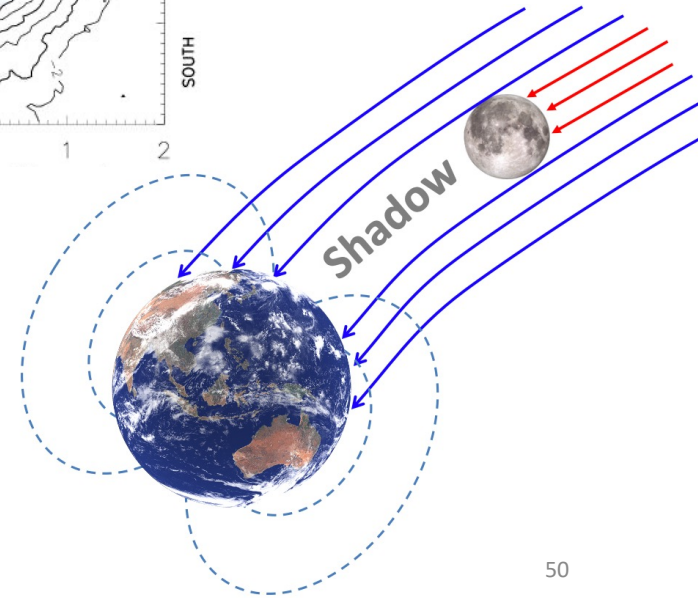


# Moon Shadow as a Calibration Source

- ✓ **Absolute Energy Scale**
  - Energy dependence of E-W displacement
- ✓ **Pointing Accuracy**
  - N-S displacement
- ✓ **Angular Resolution**
  - Deficit Shape
- ✓ **Detector Stability**
  - Temporal variation
- ✓ **Anti- $P$  /  $P$  Ratio**
  - Opposite-side deficit



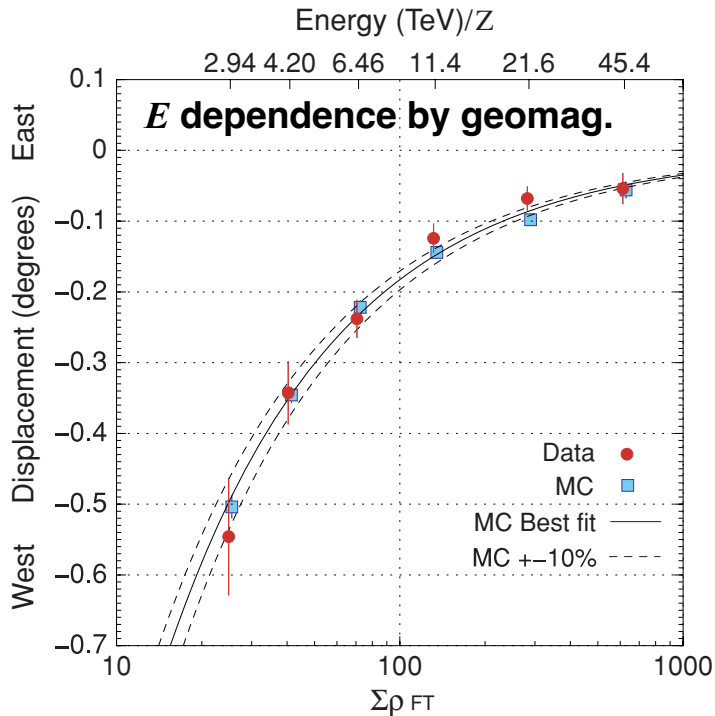
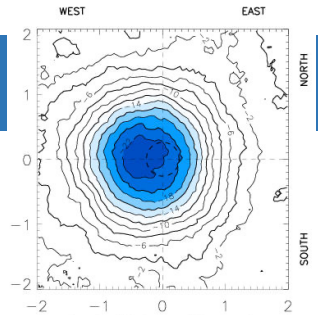
$$\Delta\theta \sim \frac{1.6^\circ}{E[\text{TeV}]}$$



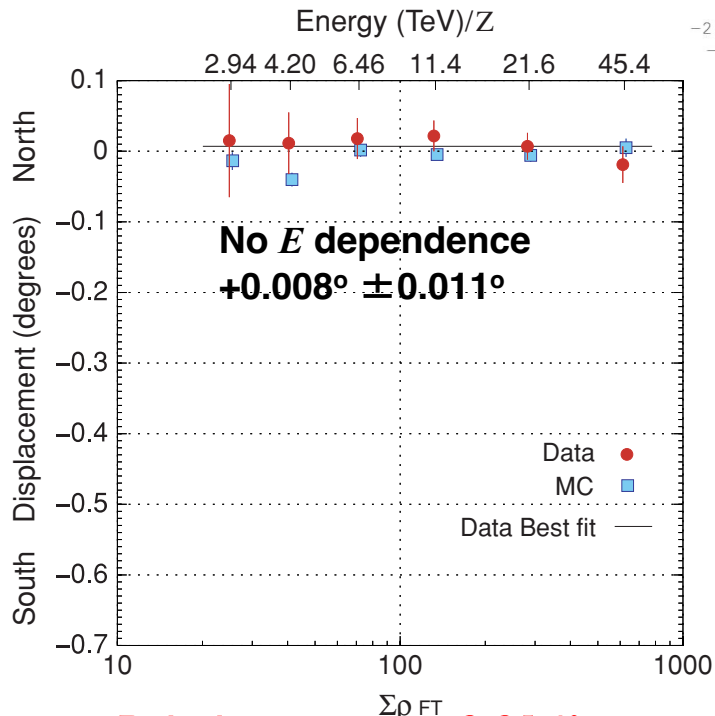


# Moon Shadow as a Calibration Source

✓ Tibet AS $\gamma$  experiment first time utilized the Moon shadow as the absolute energy calibration.



**Absolute  $E$  error =  $\pm 12\%$**   
**Best-fit =  $-4.5\% (\pm 8.6\text{stat.} \pm 6.7\text{sys.})\%$**



**Pointing error =  $\pm 0.014^\circ$**   
*Amenomori et al., ApJ (2009), ICRC2005*